Master Thesis
Space Time Codes for Massive MIMO

S.V.V.RACHURI

TU Delft

Delft
University of
Technology

Challenge the future
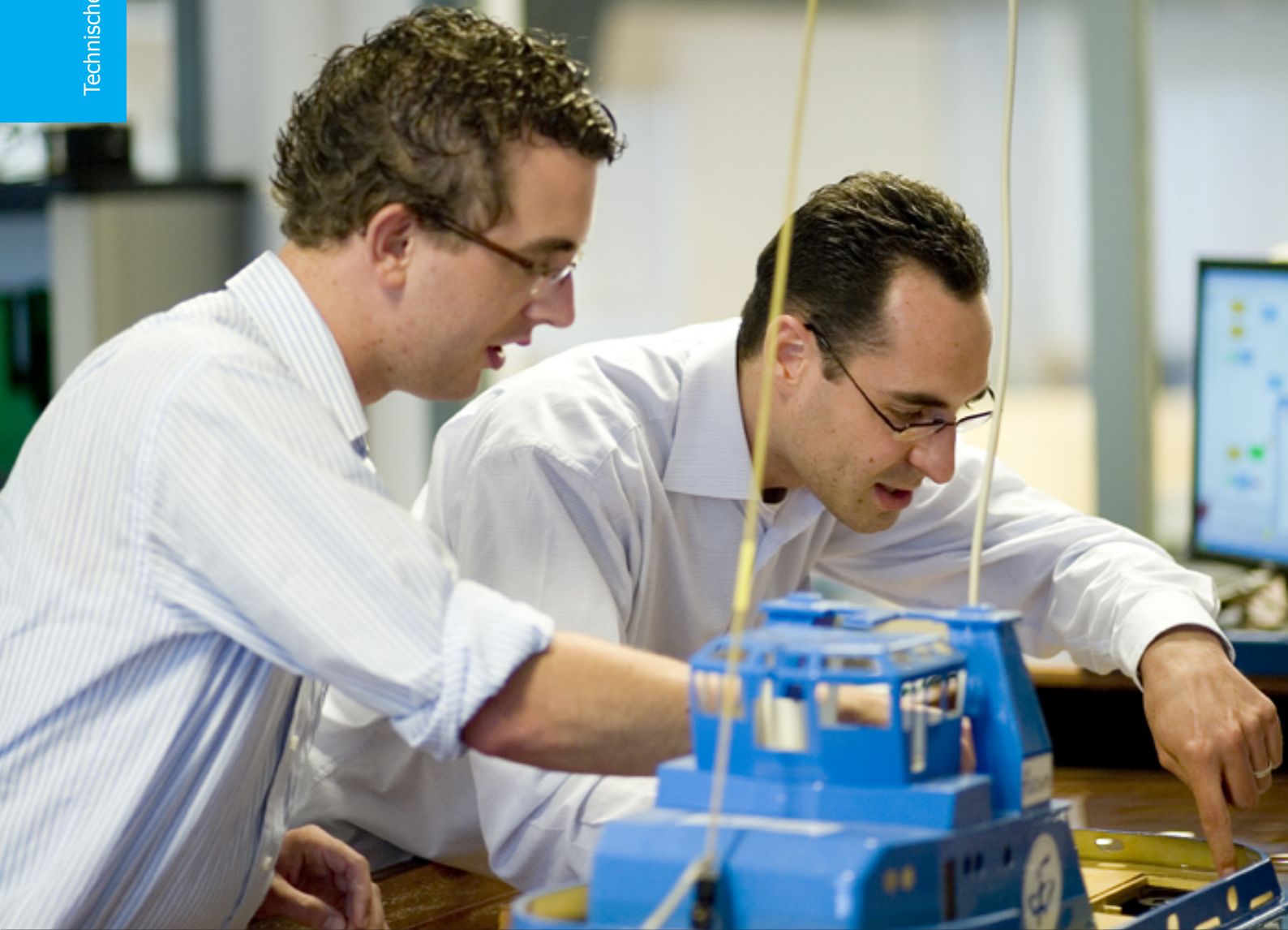
SPACE TIME CODES FOR MASSIVE MIMO SYSTEMS

A thesis submitted to the Delft University of Technology in partial fulfillment
of the requirements for the degree of

Master of Science in Telecommunication and Sensing Systems

by

Vishnu Vardhan RS

December 6, 2019

Student Number: 4734335

Thesis Committee : prof.dr.ir. G.J.T. Leus, TU Delft
Dr.ir. Jos Weber, TU Delft
Prof.Dr.ir. Sofie Pollin, KU Leuven

ABSTRACT

Ubiquitous connectivity requirements and stringent quality-of-services (QoS) in recent wireless communications demand new revolutionary wireless network technologies to support the exponentially increasing traffic growth. Massive multiple-input-multiple-output (MIMO) with the capability of high spectral efficiency achieved by large multiplexing and diversity gains grabbed a lot of attention as a promising solution for future cellular networks. Achieving ultra-reliable and low latency communication is very challenging without increasing the network infrastructure cost, or extra processing complexity. Adapting space-time-block-codes (STBC) can improve the reliability of the system, but this increases the downlink pilot overhead. Two precoders are devised to exploit full spatial diversity with the blind combining process to avoid downlink pilot overhead.

Many researchers explored combining beamforming with STBC to exploit multiplexing and diversity gain to suppress interference and enhance reliability. Downlink precoder is devised by utilizing channel knowledge and mentioned gains, to suppress interference at the Base Station (BS) thus reducing the post-processing complexity at the receiver. Orthogonal beams to the interference channels are constructed using eigenvalue decomposition to superimpose STBC branches to exploit spatial multiplexing and diversity gain. However, to coherently decode the symbols instantaneous channel state information or statistical channel knowledge is required. Obtaining channel knowledge at the receiver demands downlink pilots, which reduces the overall spectral efficiency. Temporal analysis of the channels is conducted to analyze the impact of the dynamic nature of the channel and its effect on the frequency of downlink pilots is studied. Robustness of the precoder under imperfect channel knowledge is also examined.

Obtaining channel knowledge is a resource-consuming process, space-time-line-codes (STLC) contributed a novel approach to achieve full spatial diversity with a blind decoding process, with the help of two receive antennas. This new decoding process reduced the computational complexity by 75 % compared to conventional STBC. Acclimating STLC into a Massive MIMO scenario and an optimal strategy to accommodate multiple users is investigated. An alternative STLC structure to achieve full spatial diversity with a single receive antenna is proposed. The performance of proposed precoders under imperfect channel knowledge is also examined. New precoders provide a very efficient encoding and decoding strategies to exploit full spatial diversity, and also exhibit better resilience under imperfect channel knowledge.

ACKNOWLEDGEMENTS

I would like to express my gratitude towards my supervisors Prof. Geert Leus, TU Delft, and Prof. Sofie Pollin, KU Leuven for their continuous support, guidance and valuable inputs during my thesis. I would also like express my special thanks to Prof.Jos Weber, TU Delft for kindly accepting to be part of my thesis committee.

Besides my supervisors, my sincere thanks to Andrea for her patience, motivation, insightful comments and especially her suggestions in writing this thesis are very insightful.

I would like to thank my colleagues at ESAT, KU Leuven for their precious support in providing necessary facilities. Without their precious assistance, it would not be possible to conduct this research.

Finally my sincere gratitude towards my family: my parents, my sister and my friends for their constant support and love . . .

CONTENTS

LIST OF FIGURES

ACRONYMS AND NOTATIONS

ACRONYMS

BS   Base Station
UE   User Equipment
mMIMO   Massive Multiple Input Multiple Output
UL   Uplink
DL   Downlink
TDMA   Time Division Multiple Access
FDMA   Frequency Division Multiple Access
SDMA   Space Division Multiple Access
TDD   Time Division Duplexing
STBC   Space Time Block Codes
STLC   Space Time Line Codes
ZF   Zero Forcing
RZF   Regular-Zero Forcing
BF   Beamforming
MMSE   Minimum Mean Square Error
CSI   Channel State Information
CHE   Channel Estimation Error
BER   Bit Error Rate
P_{out} Outage Probability
d_{out} Overall Diversity
QPSK   Quadrature Phase Shift Keying
SVD   Singular Value Decomposition
SINR   Signal to Interference and Noise Ratio
SNR   Signal to Noise Ratio

NOTATIONS

Vectors and Matrices are represented by bold letters, where small bold letters ($\mathbf{x}$) corresponds vectors and ($\mathbf{X}$) corresponds to matrices.

$\log(.)$	Natural logarithm
$log_2(.)$	Base 2 logarithm
x^*	Complex conjugate of x
$|x|$	Absolute value of scalar
$\mathbb{E}\{.\}$	Expectation Operator
$[.]^T$	Transpose Operator
$[.]^H$	Hermitian(Complex Conjugate) Operator
$\mathbf{X}^{-1}$	Inverse Operator for Matrix
$\mathbf{I}_n$	Identity Matrix of size n
$\mathbf{0}_n$	Zero Matrix of size n
$\|\mathbf{x}\|$	Eucledian Norm of vector $\mathbf{x}$
$\Re\{x\}$	Real part of x
$\Im\{x\}$	Imaginary part of x
$\mathbf{X}^\dagger = (\mathbf{X}^H\mathbf{X})^{-1}\mathbf{X}^H$	Pseudo-Inverse of matrix $\mathbf{X}$

1 | INTRODUCTION

The rapid increase in connectivity between various applications through mobile networks is pushing the limits for higher data rates and Quality of Services (QoS). Future networks must be comprised of three generalized features: 1) ubiquitous connectivity 2) extremely low latency and 3) high-speed data transfer. According to the European research community for 5G, Horizon 2020, three main use cases are divided for future 5G networks [1].

1.1 USE CASES OF 5G:
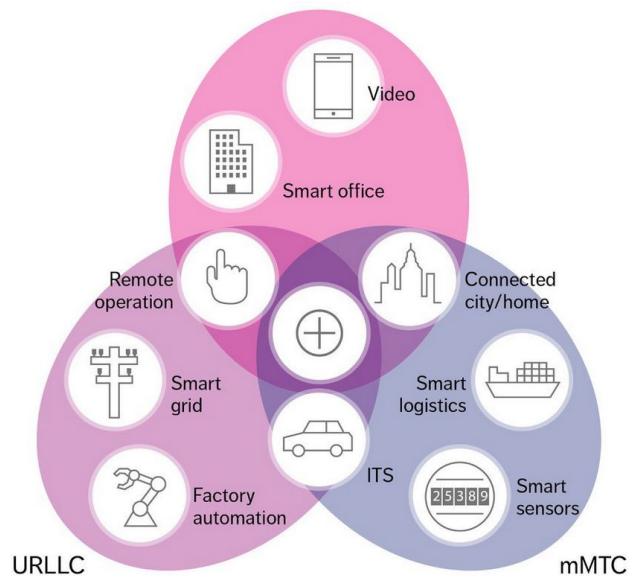
Figure 1.1: Use cases of 5G.

- Enhanced Mobile Broadband: The increase of applications like augmented reality, virtual reality, and health-related applications necessitates achieving higher data rates along with more spectrum. To meet the requirements of future internet a lot of research is going on in the direction of techniques like mm-Waves, Massive MIMO (Multiple Input Multiple Output), carrier aggregation and new waveforms to increase the spectral efficiency.

- Massive Machine Type Communication: Increase in large scale distributed communication devices, which sporadically transmit small data packets, like smart grids, sensor networks, endless Internet of Things (IoT) devices, etc, demand future networks to support the aggregated traffics along with minimizing the energy consumption to

extend the lifetime of the systems [2]. As some of these devices might be placed in harsh environments, massive Machine Type Communication (mMTC) should consider these aspects as well.

- Ultra Reliable Low Latency: Introduction of applications like self-driving vehicles and health applications like remote surgery and remote monitoring through wearables induces stringent requirements like availability of 99.9999%, BER of 10^{-9} and latencies approaching 1ms [3], this use case is also called Mission Critical Communication(MCC).

These new requirements compel us to redefine conventional cellular networks. Massive MIMO is one of the proposed solutions towards handling increasing data rates, increasing network capacity, massive device support, energy efficiency, and interference management [11].

1.2 MASSIVE MIMO:

Massive MIMO with beamforming capabilities improves the effectiveness of the transmission and end-user experience by significantly increasing network capacity and coverage while also reducing interference. Base Stations equipped with more number of antennas, can form multiple beams, which could serve multiple users in parallel using the same space and time resources, which is also known as spatial multiplexing. One of the first works about Massive MIMO by T.Marzetta [4] inspired many researchers to explore Massive MIMO technologies and its challenges, which provided impressive solutions towards spectral efficiency. These results grabbed a lot of attention in telecommunication giants like Ericsson, Nokia, and Huawei to commercially deploy BSs (Base Stations) supporting multiple antennas [11].

1.3 SPACE TIME BLOCK CODES:

Wireless communication systems face new challenges in reliably conveying information to the receiver in the presence of fading channels. A natural solution to improve the performance is to ensure that the data symbols pass through multiple paths, where each path has independent fading, also known as diversity, and this proved to be a promising technique to combat fading [21].

As time/frequency resources are scarce, spatial diversity is extremely useful compared to time diversity and frequency diversity. A Space-Time Block Codes (STBC) robust transmit diversity technique (refer Figure 1.2), which could exploit spatial diversity as well as temporal diversity, and can improve the reliability of transmission without the knowledge of channel state information by increasing the effective SNR (Signal to Noise Ratio) at the receiver.

1.4 MOTIVATION OF THE THESIS:

Space-Time Codes are adapted into a Massive MIMO scenario in [6],[7] and [8]. These studies considered a perfect CSI (Channel State Information) at the receiver to coherently decode the received symbols. A general technique
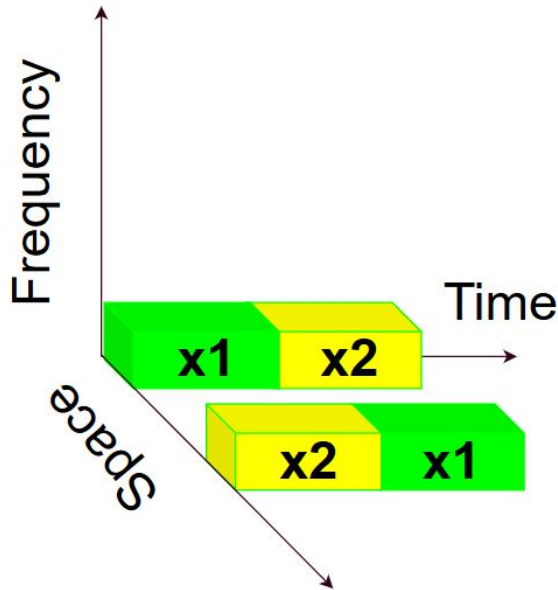
Figure 1.2: Typical Space-Time Block structure.

is to form multiple orthogonal beams using the eigen vectors of the correlation matrix of the estimated channel at the Base Station (BS) and using them as diversity branches to superimpose space-time codes provided a significant improvement in the performance.

It is a well-established fact that obtaining channel state information in massive MIMO is a very resource-consuming process as well as computationally challenging. Especially at downlink, receiver estimating CSI of M transmitting antennas is unfavorable and affects the whole performance of the receiver, exploring CSI independent decoding techniques are advisable. The main objective of this thesis is to achieve a computationally optimal novel precoder design to exploit full spatial diversity with CSI independent decoding.

Space-time line codes proposed in [9] provided an optimal code design to exploit full spatial diversity along with reducing the computational complexity as well as channel-independent decoding. Inspired by the contributions of this work new techniques are explored to accommodate multiple users.

The performance of these precoders are analyzed via the following factors:

- Bit Error Performance of Single User and Multi-User scenarios.

- How channel uncertainty is affecting the performance.

- How computationally effective the precoder is.

Current cellular networks demands huge spectral efficiency, finding an optimal precoder which could exploit multiplexing gain as well as spatial diversity gain by removing the demand of *Downlink pilots* is highly advisable.

1.5 OUTLINE OF THE THESIS:

This section discusses outline of this thesis:

Chapter 2 explains the uplink and the downlink system model for massive MIMO systems. The spatial correlation model along with channel estimation techniques are discussed. Wireless channels are more dynamic in nature and their behavior under mobility scenarios are always of great interest, in order to determine how swiftly the channel becomes significantly different, temporal analysis on a radially moving user is determined.

Chapter 3 is devoted to discussing the spatial diversity and how spatial diversity can improve the performance of massive MIMO systems. This discussion starts with explaining diversity techniques, space-time block codes, diversity in massive MIMO systems and Diversity-Multiplexing trade-offs. Exploiting both beamforming gain and diversity gains are widely discussed. The performance of such precoder is analyzed. Channel knowledge at receiver plays a major role in coherent decoding of symbol. In order to analyze the frequency of downlink pilots required coherent time analysis is considered.

Chapter 4 introduces Space Time Line Codes (STLC), achieving full spatial diversity along with channel-independent blind combining schemes to decode the desired symbols. Antenna allocation strategies are introduced to accommodate multiple users, but this is not an optimal solution as each user cannot exploit full antenna array gain. Two novel integrated STLC precoders with the help of Zero-Forcing coefficients are proposed to accommodate multiple users, and their performance is analyzed under imperfect channel knowledge conditions. A brief analysis of computational complexity evaluation is also included.

Chapter 5 gives a brief summary of important conclusions and highlights observed in this thesis, along with possible future research directions.

2 | MASSIVE MIMO

This chapter discusses the basic concepts related to massive MIMO systems.

The fundamental anticipation from massive MIMO systems is to magnify the benefits of conventional MIMO systems on a greater scale. Compared to single antenna systems, distinctive property of antenna array to focus the energy in certain directions as beams, opened a new gateway towards spatial-division multiplexing [11].

Multiple access technique allows multiple users to exploit resources like frequency, time and space to increase the capacity with achieving a sufficient level of quality of service. In contrast to contemporary TDMA, FDMA systems, where different time resources and frequency resources are occupied respectively to accommodate multiple users, SDMA allows the users to utilize both time and frequency resources simultaneously as conceptually shown in Figure 2.1.

(a) Time Division Multiple Access. **(b)** Frequency Division Multiple Access.

(c) Space Division Multiple Access.
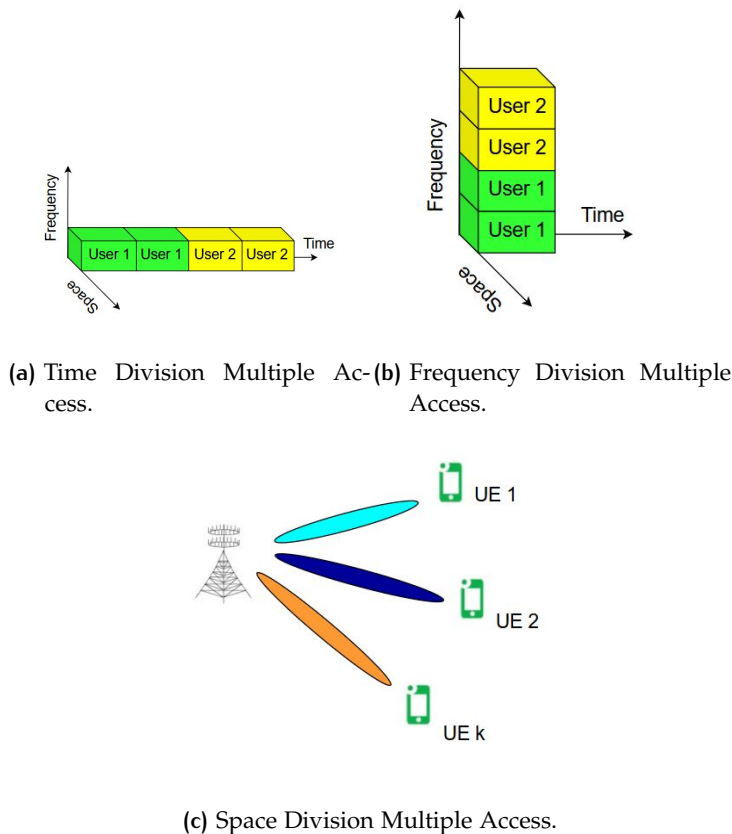
Figure 2.1: Various multiple access techniques.

In [12],[13] for the first time, antenna arrays with the help of spatial processing techniques to discriminate signals from different users in the uplink, *receive combining* and in downlink, *transmit precoding* are discussed.
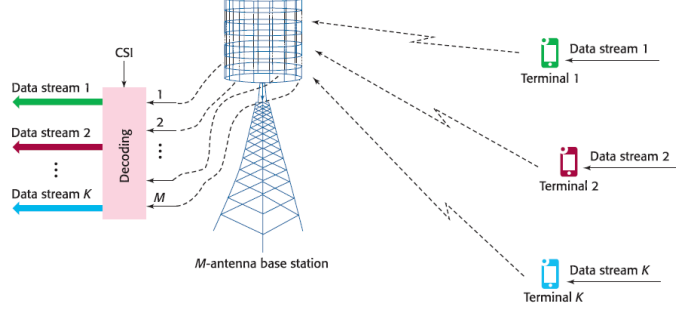
Figure 2.2: Uplink model for Massive MIMO.

2.1 MASSIVE MIMO SYSTEM MODEL FOR UPLINK AND DOWNLINK:

Consider a mMIMO network with L cells operating on Time Division Duplex (TDD) where each BS j with M_j antennas and K_j users, where $M_j \gg 1$ and antenna-UE ratio $M_j/K_j > 1$. Uplink model for mMIMO can be exemplified as shown in Figure 2.2 and UL signal can be modelled as $\mathbf{y}_j \in \mathbb{C}^{M_j}$, where $\mathbf{h}_{j,k}^j \in \mathbb{C}^{M_j \times 1}$ corresponds to channel k-th user in cell j and BS lies in cell j, $s_{j,k}$ represents the information of k-th user in cell j and $\mathbf{n}_j \sim \mathcal{N}_\mathbb{C}\left(\mathbf{0}_{M_j}, \sigma_{UL}^2 \mathbf{I}_{M_j}\right)$, where $\mathbf{I}$ represents an identity matrix, independent additive white Gaussian noise with zero mean and variance σ_{UL}^2.

$$\mathbf{y}_j = \underbrace{\sum_{k=1}^{K_j} \mathbf{h}_{jk}^j s_{j,k}}_{Desired Signals} + \underbrace{\sum_{l=1,l\neq j}^{L} \sum_{i=1}^{K_l} \mathbf{h}_{li}^j s_{l,i}}_{Inter-cell Interference} + \underbrace{\mathbf{n}_j}_{Noise} \tag{2.1}$$

BS in cell j selects $\mathbf{v}_{jk} \in \mathbb{C}^{M_j}$, *combining* vector of k-th user in j-th cell for each user to separate the desired signals.

$$\mathbf{v}_{jk}^H \mathbf{y}_j = \underbrace{\mathbf{v}_{jk}^H \mathbf{h}_{jk}^j s_{jk}}_{Desired signal} + \underbrace{\sum_{i=1,i\neq k}^{K_j} \mathbf{v}_{jk}^H \mathbf{h}_{ji}^j s_{ji}}_{Intra-cell Interference}$$
$$+ \underbrace{\sum_{l=1,\neq j}^{L} \sum_{i=1}^{K_l} \mathbf{v}_{jk}^H \mathbf{h}_{li}^j s_{li}}_{Inter-Cell Interference} + \underbrace{\mathbf{v}_{jk}^H \mathbf{n}_j}_{noise} \tag{2.2}$$

Similarly, downlink can be modelled as (2.3)

$$\mathbf{x_l} = \sum_{i=1}^{K_l} \mathbf{w}_{li} \zeta_{li} \tag{2.3}$$
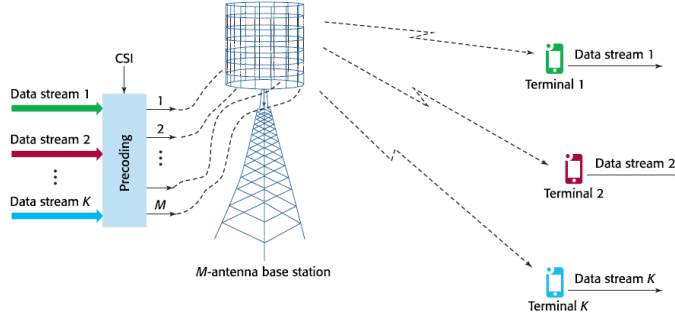
Figure 2.3: Downlink model for Massive MIMO.

where the *precoding* vector $\mathbf{w}_{lk} \in \mathbb{C}^{M_l \times 1}$ determines the spatial directivity of transmission. The received signal at k-th user in cell j represented as (2.4) and ζ_{li} represents the information of i-th user in l-th cell.

$$y_{j,k} = \sum_{l=1}^{L} \left(\mathbf{h}_{jk}^{j}\right)^{H} \mathbf{x}_l + n_{jk} \tag{2.4}$$

Propagation channels between BS and UEs change over time and frequency, transmitted signal over a given time interval is spreads out and received over a longer duration. Considering a bandwidth of B, the time interval between samples decrease as B increases. The classic solution is to divide a bandwidth, B, into multiple narrow-band sub-carriers resulting in effective time interval between samples longer than channel dispersion, which makes the subcarrier channels easy to estimate.

A *coherence block* consists of a number of flat fading subcarriers over which channel response is approximated as constant. Each coherence block consists of $\tau_c = B_c T_c$ samples, where B_c and T_c corresponds to *coherence bandwidth* and *coherence time* respectively. Each *coherence block* assumed to have random channel response which are statistically independent to other blocks. Operating in TDD mode each coherence block is divided to serve both UL(Uplink) and DL(Downlink) $\tau_c = \tau_{UL-Pilot} + \tau_{UL-Data} + \tau_{DL-Pilot} + \tau_{DL-Data}$ [11].

2.2 SPATIAL CORRELATION MODEL:

Operating on TDD mode allows channel response ($\mathbf{h}_{jk}^{j}$) between k-th user in j-th cell and BS is in j-th cell is same in both UL and DL. BS has many antennas, where each antenna has a non-uniform radiation pattern which makes some spatial directions carry stronger signals from BS to UE.

Correlated Rayleigh fading channels are represented as $\mathbf{h}_{jk}^{j} \sim \mathcal{N}_{\mathbb{C}}\left(\mathbf{0}_{M_j}, \mathbf{R}_{jk}^{j}\right)$, where $\mathbf{R}_{jk}^{j}$ represents positive semi-definite spatial correlation matrix. Spatial channel correlation method is the most important property of Multi-User Massive MIMO, local scattering model is considered and spatial correlation matrix (to compute correlation matrix indices are removed to simplify this process) $\mathbf{R} \in \mathbb{C}^{MxM}$ is modelled as $\mathbf{R} = \mathbb{E}\left\{\sum_{n=1}^{N_{path}} \mathbf{a}_n \mathbf{a}_n^{H}\right\}$ where $\mathbf{a}_n \in \mathbb{C}^{M}$ is represented as (2.7), where $g_n \in \mathbb{C}$ represents gain and phase

rotation of the path and d_H corresponds to antenna spacing. The channel response $\mathbf{h}$ is considered as the superposition of N_{path} components [14] [15].

$$\mathbf{h} = \sum_{n=1}^{N_{path}} \mathbf{a}_n \tag{2.5}$$

Angles $\bar{\varphi}_n$ represents i.i.d. random variables with angular probability density function $f(\bar{\varphi}_n)$ and g_n represents i.i.d. random variables with zero-mean and variance $\mathbb{E}\left\{|g_n|^2\right\}$

$$\mathbf{h} \to N_{\mathbb{C}}\left(\mathbf{0}_M, \mathbf{R}\right), N_{path} \to \infty \tag{2.6}$$

Assuming a lack of scattering around the BS, it is reasonable to assume that all the multipath components originate from a scattering cluster around the UE, which refers to the local scattering model. Where $\bar{\varphi} = \varphi + \delta$ represents φ angle of arrival and δ is random deviation, Gaussian distributed $\delta \sim \mathcal{N}\left(0, \sigma_\varphi^2\right)$. In this article *one-ring* model assuming all scatterers lie on a circle centering the UE, where random deviations follow uniformly distributed $\delta \sim \mathcal{U}\left(-\sqrt{3}\sigma_\varphi, \sqrt{3}\sigma_\varphi\right)$ [15,16].

$$\mathbf{a}_n = g_n \begin{bmatrix} 1 & e^{j2\pi d_H sin(\bar{\varphi}_n)} & ... & e^{j2\pi d_H(M-1)sin(\bar{\varphi}_n)} \end{bmatrix} \tag{2.7}$$

Correlation matrix is defined as $\mathbb{E}\left\{\sum_n \mathbf{a}_n \mathbf{a}_n^H\right\}$, can be mathematically modelled as:

$$[\mathbf{R}]_{l,m} = \sum_{n=1}^{N_{path}} \mathbb{E}\left\{|g_n|^2\right\} \mathbb{E}\left\{e^{2\pi jd_H(l-1)sin(\bar{\varphi}_n)} e^{-2\pi jd_H(m-1)sin(\bar{\varphi}_n)}\right\} \tag{2.8}$$

$$= \beta \int e^{2\pi jd_H(l-m)sin(\bar{\varphi})} f(\bar{\varphi}) d\bar{\varphi} \tag{2.9}$$

$\mathbf{R}$ is a Toeplitz matrix, as $[\mathbf{R}]_{l,m}$ depends on the difference of $l - m$ and $\beta = \sum_{n=1}^{N_{path}} \mathbb{E}\left\{|g_n|^2\right\}$ corresponds to average path gain.

2.3 CHANNEL HARDENING AND FAVOURABLE PROPAGATION :

Wireless channels suffers due to random fluctuations in the propagation environment, this is also often referred as small-scale fading. Multiple antennas at BS can offer spatial diversity to combat this by making this fading channel behave as deterministic channel, is also known as **Channel Hardening**. The definition says that the gain of arbitary fading channel is close to the mean value (2.11) [11] .

$$\frac{\left\|\mathbf{h}_{jk}^j\right\|^2}{\mathbb{E}\left\{\left\|\mathbf{h}_{jk}^j\right\|^2\right\}} \to 1 \tag{2.10}$$

Where **Favorable Propagation** measures the orthogonality of UEs the channels , UEs with asymptotically orthogonal channels indeed mitigate the interference between UEs.

$$\frac{(\mathbf{h}_{li}^{j})^{H}\mathbf{h}_{jk}^{j}}{\mathbb{E}\left\{\left\|\mathbf{h}_{jk}^{j}\right\|^{2}\right\}\mathbb{E}\left\{\left\|\mathbf{h}_{li}^{j}\right\|^{2}\right\}} \rightarrow 0 \tag{2.11}$$

2.4 CHANNEL ESTIMATION:

BS needs to estimate channel response from the active users within coherence block, minimum mean-squared error (MMSE) estimator is considered to estimate the channel using UL pilot symbols. Each pilot sequence of k-th user in j-th cell, $\boldsymbol{\phi}_{j,k} \in \mathbb{C}^{\tau_p}$, spans τ_p samples. $\boldsymbol{\phi}_{j,k}$ are scaled to satisfy the constant power constraints leading to received signal as $\mathbf{Y}_j^p \in \mathbb{C}^{M_j \times \tau_p}$, where $\mathbf{N} \in \mathbb{C}^{M_j \times \tau_p}$ is Additive White Gaussian Noise (AWGN) normally distributed with zero mean and σ_{UL}^2 variance.

$$\mathbf{Y}_j^p = \underbrace{\sum_{k=1}^{K_j}\mathbf{h}_{jk}^{j}\boldsymbol{\phi}_{jk}^{T}}_{Desired\,Pilots} + \underbrace{\sum_{l=1,l\neq j}^{L}\sum_{i=1}^{K_l}\mathbf{h}_{li}^{j}\boldsymbol{\phi}_{li}^{T}}_{Inter-cell\,pilots} + \underbrace{\mathbf{N}_j^p}_{Noise} \tag{2.12}$$

To successfully estimate the channel coefficients these pilot sequences should be deterministic and known at BS, using *channel reciprocity* downlink channel is presumed. $y_{jjk}^p \in \mathbb{C}$ in (2.13) is the correlated sequence of k-th user in j-th cell and BS in j-th cell, using $\boldsymbol{\phi}_{jk}$ can be approximated as $\hat{\mathbf{h}}_{jk}^{j}$ (estimated channel coefficients) has the same dimension as $\mathbf{h}_{jk}^{j}$ [17].

$$\mathbf{y}_{jjk}^p = \mathbf{Y}_j^p\boldsymbol{\phi}_{jk}^{*}$$
$$= \underbrace{\sum_{k=1}^{K_j}\mathbf{h}_{jk}^{j}\boldsymbol{\phi}_{jk}^{T}\boldsymbol{\phi}_{jk}^{*}}_{Desired\,Pilots} + \underbrace{\sum_{i=1,i\neq k}^{K_j}\mathbf{h}_{ji}^{j}\boldsymbol{\phi}_{ji}^{T}\boldsymbol{\phi}_{jk}^{*}}_{Intra-cell\,pilots} + \underbrace{\sum_{l=1,l\neq j}^{L}\sum_{i=1}^{K_l}\mathbf{h}_{li}^{j}\boldsymbol{\phi}_{li}^{T}\boldsymbol{\phi}_{jk}^{*}}_{Inter-cell\,pilots} + \underbrace{\mathbf{N}_j^p\boldsymbol{\phi}_{jk}^{*}}_{Noise}$$

$$\tag{2.13}$$

Second and third term in (2.13) represents interference contributed from desired UE and other UEs existing in the same cell and other cells. If every UE is allocated with orthogonal pilot sequences makes these interference terms vanish. Pilot sequences are τ_p dimensional vectors, τ_p mutually orthogonal pilot sequences are used to form a pilot book $\boldsymbol{\Phi} \in \mathbb{C}^{\tau_p \times \tau_p}$, where $\boldsymbol{\Phi}^H\boldsymbol{\Phi} = \tau_p\mathbf{I}_{\tau_p}$. BS allocates different pilot sequences to different UEs, so coordination of pilot assignment across cells is very important. $\mathcal{P}_{jk}$ represents a set of indices which uses the same pilot sequence as $\boldsymbol{\phi}_{j,k}$ [18] [19].

2.4.1 Minimum Mean Square Error Channel Estimator

(2.13) represented how $\mathbf{Y}_j^p$ received pilot sequence. Minimum Mean Square Error of $\mathbf{h}_{li}^j$ is $\hat{\mathbf{h}}_{li}^j$ is derived such that it minimizes $\mathbf{E}\left\{\left\|\mathbf{h}_{li}^j - \hat{\mathbf{h}}_{li}^j\right\|^2\right\}$. Recalling the UL pilot sequences received in (2.13) channel estimates are derived:

$$\hat{\mathbf{h}}_{li}^j = \sqrt{p_{li}}\mathbf{R}_{li}^j\Psi_{li}^j\mathbf{y}_{jli}^p \tag{2.14}$$

$$\Psi_{li}^j = \left(\sum_{(l',i')\in\mathcal{P}_{li}} p_{l'i'}\tau_p\mathbf{R}_{l'i'}^j + \sigma_{UL}^2\mathbf{I}_{M_j}\right)^{-1} \tag{2.15}$$

MMSE estimates $\hat{\mathbf{h}}_{li}^j$ and estimation errors are $\tilde{\mathbf{h}}_{li}^j = \mathbf{h}_{li}^j - \hat{\mathbf{h}}_{li}^j$ are independent random variables normally distributed. Where $\mathbf{C}$ corresponds to estimation error correlation matrix and $\mathbf{R}$ channel correlation matrix.

$$\hat{\mathbf{h}}_{li}^j \sim \mathcal{N}_{\mathbf{C}}\left(\mathbf{0}_{M_j}, \mathbf{R}_{li}^j - \mathbf{C}_{li}^j\right)$$
$$\tilde{\mathbf{h}}_{li}^j \sim \mathcal{N}_{\mathbf{C}}\left(\mathbf{0}_{M_j}, \mathbf{C}_{li}^j\right) \tag{2.16}$$
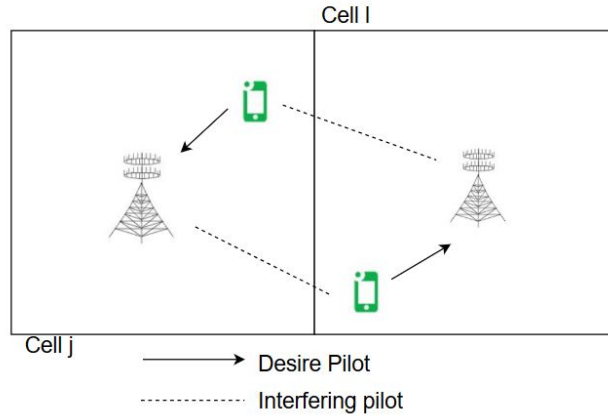
Figure 2.4: UEs in cell l and cell j using same pilot sequence results in pilot contamination.

More reliable channel estimates can be obtained as $tr(\mathbf{C}_{li}^j)$ decreases, $tr(\mathbf{C}_{li}^j) = 0$ results in perfect estimates. UEs transmitting same pilot sequences has a negative impact on gaining true channel realizations, this is also known as *pilot contamination*. Figure 2.4 depicts the pilot contamination, which results as a limiting factor in obtaining quality channel estimates and results in an inability to suppress the interference between UEs using same pilot sequences [20]. In this article MMSE channel estimator is used for channel estimation at BS.

According to the availability of CSI massive MIMO systems are classified into:

- Closed loop massive MIMO system: Closed loop systems obtains the information of channel gain and phase from the receiver. Channel

State Information (CSI) is available at both the transmitter and the receiver. CSI could be of two types instantaneous channel and statistical average of the channel [21].

- Open loop massive MIMO system: Open loop systems has receiver estimating the channel using pilot signals but no feedback is given to the transmitter. Hence CSI is available at only one end not at both terminals.

- Blind massive MIMO system: In blind MIMO system, no channel state information is available at both the transmitter and the receiver.

2.5 TEMPORAL ANALYSIS OF CHANNEL:

Real-time scenarios involve offering services to users with high mobility and it is of great interest to investigate the evolution of massive MIMO channels under more dynamic scenarios. Using synchronous TDD systems where the channel state information at the transmitter estimated by UL training pilots. This more dynamic nature of channel generated huge attention on how correlated channels are over time and how quickly the channel becomes significantly different.

To assess the temporal changes in multi-antenna channels under mobility for these time dependent simulated channels time correlation function (TCF), for i-th user and r-th simulation is derived as Equation 2.17 [22].

$$TCF_i\left(\tau\right) = \frac{\mathbf{E}\left\{\left|\mathbf{h}_{i,r}\left[t-\boldsymbol{\tau}\right]^H \mathbf{h}_{i,r}\left[t\right]\right|\right\}}{\mathbf{E}\left\{\left|\mathbf{h}_{i,r}\left[t\right]^H \mathbf{h}_{i,r}\left[t\right]\right|\right\}} \tag{2.17}$$

To evaluate how quickly channel decorrelates over time with varying speeds a closest real-time scenario is modeled.
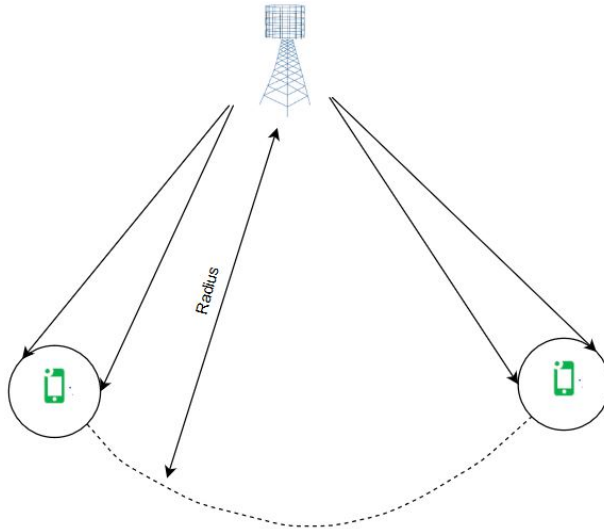
Figure 2.5: Considered user mobility scenario.

2.6 MODELLING THE SIMULATED ENVIRONMENT:

To epitomize the closest real time scenario, we analyze the performance of square pattern cells, with each cell area $(0.25km \times 0.25km)$, simulation parameters are listed in Table 2.1 [23].

Table 2.1: System parameters chosen for Simulations

Index	Parameter	Symbol	Value
1	No.of BS antennas	M_{Tx}	128
2	(No.of UE antennas)	N	1
3	(No.of Users/cell)	K	4
4	Pathloss exponent	α	3.76
5	Shadow fading	σ	= 10
6	Number of cells	L	1
7	Channel Model		One-Ring
8	Angular Standard Deviation	σ_φ	$10°$

Figure 2.5 represents radially moving users with varying speeds of 1, 5, 10, 15 and 20 Degree/Sec (0.88, 4.3, 8.7, 13.1 and 17.5 m/sec) at a radius of 50m.
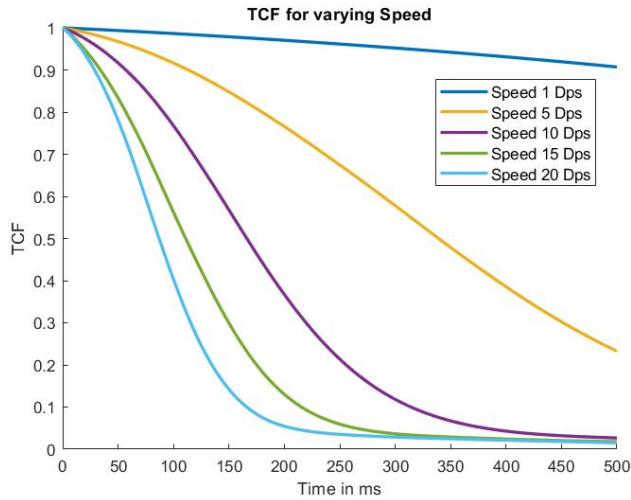
Figure 2.6: Temporal analysis of channels of UE with varying speeds.

Figure 2.6 indicates the temporal changes and how quickly channels decorrelate, users with high mobility experience more quicker decorrelation. Quality of CSI is affected by the mobility of the user,this results in shrinkage of coherence time which results in more frequent demanding of CSI.

Channel state information (CSI) is the limiting factor in communication systems with many antennas. BS needs to estimate channel response to efficiently use the large antenna array, temporal analysis showed that users with high mobility demand more frequent CSI updates.

2.7 SUMMARY

The main objective of this chapter is to introduce the Massive MIMO systems, also outlined existing subsystems used to model our communication system model to compare various proposed precoders. The channel model and channel estimation technique used are also explained. Real-time channel modeling a challenging process, to analyze the dynamic nature of the channel, a radially moving user scenario is modeled to assess how quickly channels decorrelate and become significantly different. This temporal analysis plays a major role in determining channel estimation periodicity. Temporal analysis showed that the quicker users started moving, the quicker the channel started becoming insignificant, and the frequency of channel estimation increases. As we are investigating new techniques to eliminate the downlink pilot overhead, this temporal analysis will help us understand how frequently BS/User has to update it's CSI.

3 | SPACE DIVERSITY: INTRODUCTION OF SPACE-TIME CODES

Transmitted signal propagates through different paths, known as *multi-path* propagation. Channel fading due to random signal attenuation and phase distortions from the Multipath Components (MPCs) results in degradation of the quality of signal. Diversity techniques, are very simple and intuitive techniques transmitting same information over multiple channels. This reduces the probability that information lost due to fading, since it would require all branches to fade simultaneously. This grabbed a lot of attention and considered to provide optimal solution to combat small scale fading [24].

Three major diversity techniques (refer to Figure 3.1):

(a) Time Diversity.   **(b)** Frequency Diversity.

(c) Space Diversity.
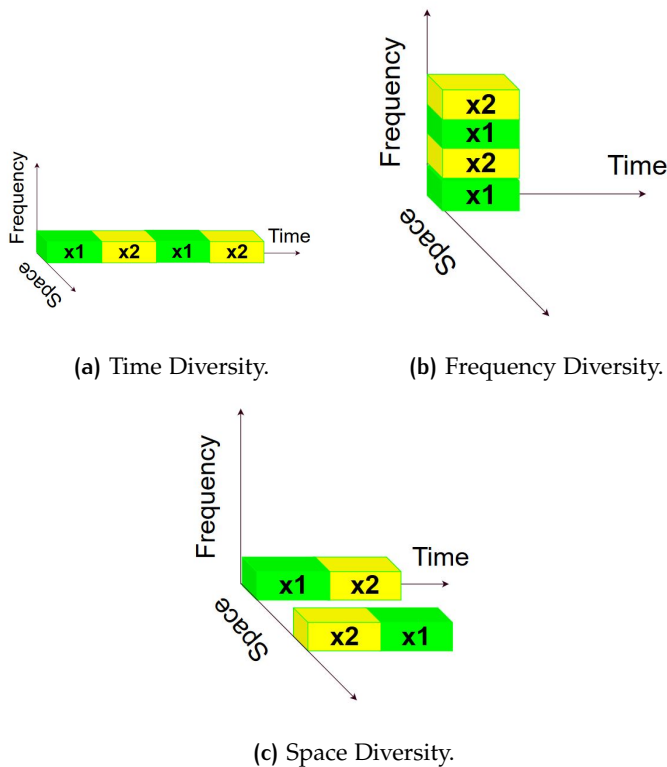
Figure 3.1: Various diversity techniques.

- Frequency diversity: Sending information by different carriers whose frequency gap is greater than coherence bandwidth, range of frequencies over which channel is constant.

- Time diversity : Sending information in different time slots which is greater than coherence time, over which channel is constant.

- Space diversity : Transmitting information through employing multiple antennas, which are separated with required inter antenna distance, at the transmitter and the receiver.

Space-Time diversity techniques demand multi-antenna systems, which significantly improves the signal quality in highly scattering environment and also boost the capacity of the channel. Receive Diversity techniques like Equal Gain Combining (EGC), Selection Combining (SC) and Maximal Ratio Combining (MRC) have been proposed and gained popularity, where as UE is generally small receive diversity is not as cost-impressive as Transmit Diversity. In this article Transmit Diversity techniques are considered as centrepiece.

Space-time codes diversify a transmitted signal through both the space and time domains. The space domain is represented by the number of transmit antennas being utilized at the BS, which allows data to be transmitted simultaneously to the receiver[21].

3.1 SPACE TIME BLOCK CODES:

Space time block code is generated by a generator matrix $\mathbf{G} \in \mathbb{C}^{M \times T}$, where M represents number of transmitting antennas and T corresponds to time slots required, aimed at achieving optimal tradeoff between spatial diversity and spatial rate and minimizing the complexity of decoder [24] :

$$
\mathbf{G} = \begin{bmatrix} g_{11} & g_{12} & \cdot\cdot & g_{1T} \\ g_{21} & g_{12} & \cdot\cdot & g_{2T} \\ . & . & .. & . \\ . & . & .. & . \\ g_{M1} & g_{M2} & \cdot\cdot & g_{MT} \end{bmatrix} \tag{3.1}
$$

Alamouti proposed a simple scheme achieving transmit diversity in [5] (Figure 3.2), using two transmitting antennas, without any loss of bandwidth, by sending two symbols over two consecutive time periods. This is also known as Space-Time Block Codes (STBC).
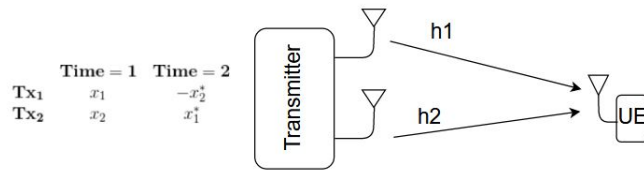
Figure 3.2: Space time block code .

$$
r_{1,1} = h_1 x_1 + h_2 x_2 + z_1
$$
$$
r_{1,2} = -h_1 x_2^* + h_2 x_1^* + z_1 \tag{3.2}
$$

$$
\begin{bmatrix} r_{1,1} \\ r_{1,2} \end{bmatrix} = \begin{bmatrix} x_1 & x_2 \\ -x_2^* & x_1^* \end{bmatrix} \begin{bmatrix} h_1 \\ h_2 \end{bmatrix} + \begin{bmatrix} z_1 \\ z_2^* \end{bmatrix} \tag{3.3}
$$

$$\begin{bmatrix} r_{1,1} \\ r_{1,2} \end{bmatrix} = \begin{bmatrix} h_1 & h_2 \\ h_2^* & -h_1^* \end{bmatrix} \begin{bmatrix} x_1 \\ x_2 \end{bmatrix} + \begin{bmatrix} z_1 \\ z_2^* \end{bmatrix} = \mathbf{H}\mathbf{x} + \mathbf{z} \tag{3.4}$$

Where z represents complex Gaussian noise term with zero mean and a variance of σ_z^2. $\mathbf{H} \in \mathbb{C}^{2\times2}$ corresponds to effective channel matrix of STBC, satisfies orthogonal property $\mathbf{H}^H\mathbf{H} = \mathbf{I}$ for optimal encoding (refer 3.3) and decoding (refer 3.5), where $\gamma_2 = |h_1|^2 + |h_2|^2$ is effective channel gain.

$$\begin{aligned} \mathbf{H}^H\mathbf{r} &= \mathbf{H}^H\mathbf{H}\mathbf{x} + \mathbf{z} \\ &= \gamma_2\mathbf{I}_2\mathbf{x} + \mathbf{z}' \end{aligned} \tag{3.5}$$

3.2 DIVERSITY IN MASSIVE MIMO AND IS STBC REQUIRED IN MASSIVE MIMO SCENARIO:

Spatial diversity gain can be defined as the measurement of link reliability and number of independent fading links as the diversity order. Quantifying diversity depends on degree of correlation between the fading coefficient random variables which they construct the massive MIMO channel matrix. High-spectral efficiency is achieved through high spatial multiplexing gain, CSI delay and estimation errors results in diversity gain losses [25]. Spatial diversity gain along with array gain and spatial multiplexing gain are known as system performance gains are improved via increasing number of antennas. But increase in more serving terminals degrades the performance gains. Link reliability is directly proportional to diversity gain, and can be measured by outage probability and Bit Error Rate(BER). Diversity measurement, D_{div}, which depends on channel correlation matrix $\mathbf{R}$ modelled as (3.6) and whole system can achieve a diversity of (3.7), where channel correlation matrices are represented as (3.8) [26].

$$D_{div}(R) = \frac{(tr(R))^2}{tr(R)^2} \tag{3.6}$$

$$D_{div-total}(R) = D_{div-DL}(R_{DL}) \times D_{div-UL}(R_{UL}) \tag{3.7}$$

$$\begin{aligned} R_{DL} &= \mathbf{E}\left\{H^H H\right\} \\ R_{UL} &= \mathbf{E}\left\{H H^H\right\} \end{aligned} \tag{3.8}$$

Spatial diversity $d_{\alpha,r}$ also depends on α channel state information quality and Spatial Multiplexing gain r. Channel coefficients are estimated at BS using uplink pilot sequences, $\hat{\mathbf{H}} = \mathbf{H} + \epsilon$. Equation 3.10 represents quantifies channel quality, where σ_ϵ^2 represents MSE(Mean Square Error) of channel estimates and ρ represents average SNR (Signal to Noise Ratio). Diversity and Multiplexing trade-offs are discussed previously in [29,30] , previous works considered to quantify diversity order via outage probabilities as it is hard to formulate PEP (Pairwise Error Probability) in massive MIMO scenarios.

Spatial multiplexing gain r depends on data rate and there exists a fundamental trade-off between multiplexing gain and diversity gain quantified as Equation 3.9 [27].

$$d_{out}(r) = (2K - M - N - 1)\, r + MN + K - K^2 + \alpha max(M, N) \qquad (3.9)$$

where $K - 1 < r \leq K \leq N$

$$\alpha = -\lim_{\rho \to \infty} \frac{log(\sigma_\epsilon^2)}{log(\rho)} \qquad (3.10)$$

Linear precoder is a promising technique to support and separate multiple users information and also provide reasonable computational complexity. Zero Forcing (ZF) and Regularized Zero Forcing (RZF) gained huge attention among these linear precoding techniques because of their ability to decouple multi user channel into independent single user channels.

$$\mathbf{W}_{Zf} = \mathbf{H}^H \left(\mathbf{H}\mathbf{H}^H \right)^{-1} \qquad (3.11)$$

$$\mathbf{W}_{RZf} = \mathbf{H}^H \left(\mathbf{H}\mathbf{H}^H + c\mathbf{I} \right)^{-1} \qquad (3.12)$$

Diversity provided by linear precoders are discussed in [28] and DMT (Diversity and Multiplexing tradeoff) is also analyzed for each linear precoder. Diversity order $d_{out}(J, N, M)$, for a spectral efficiency of J (bits/sec/Hz), M Tx antennas and N Rx antennas, is quantified on the basis of outage probability $p_{out}(J, N, M)$ rather than error analysis as mathematically calculating error probabilities are little convoluted. Equation 3.13 represents outage probability, where $I(x; y)$ represents mutual information and γ_k represents with SINR(Signal to Interference and Noise Ratio).

$$P_{out}(J, N, M) \simeq \mathbb{P}(I(x; y) < J)$$
$$\simeq \mathbb{P}(\sum_{k=1}^{K} log(1 + \gamma_k) < J) \qquad (3.13)$$
$$d_{out}(J, N, M) = -\lim_{\rho \to \infty} \frac{log(P_{out}(J, M, N)}{log(\rho)}$$

Coming to the diversity analysis under multiplexing gain ($r > 0$) system will introduce error floor as multiplexing gain increases. Figure 3.3 shows the tradeoff between diversity gain and multiplexing gain, more receiving antennas at UEs improves the overall diversity gain if multiplexing gain equals to the number of receiving antennas overall diversity reaches to zero [27].

$$d_{ZfP} = (M - N + 1)(1 - \frac{r}{N}), r \in (0, N]$$
$$d_{RZfP} = 0, r \in (0, N] \qquad (3.14)$$

Figure 3.3 demonstrated that as multiplexing gain increasing, diversity gain is affected, which further degrades the reliability. This inspired many researchers integrate Space Time Block Codes into Massive MIMO.
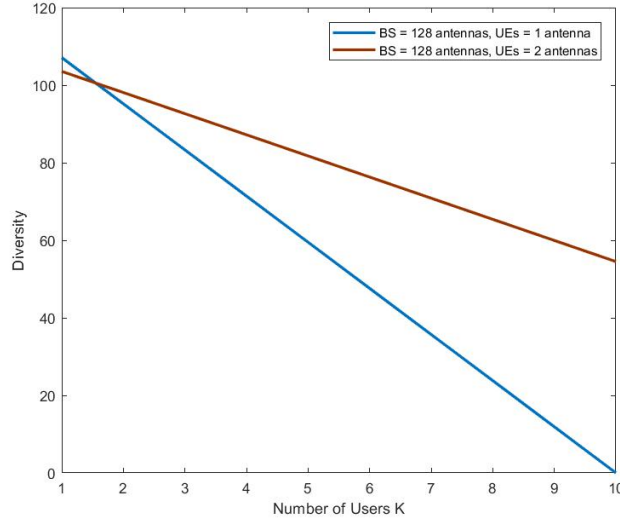
Figure 3.3: Diversity and Multiplexing Tradeoff for Zero-Forcing Precoder.

3.3 COMBINING BEAMFORMING AND STBC

The unique property of the antenna array allows the signal processing techniques to alter the field strength pattern to form variant dominant directivity by forming different *beams*. With appropriate weights and phase, precoding, for each antenna, the antenna array response can steer the direction of a signal by attenuating signals from other directions, known as *beamforming* [31]. The spatial division is used to divide the channel between each user into multiple beams onto which we can superimpose the Orthogonal Space-time Block codes so that we can exploit the beamforming and diversity gain.

Optimal precoder forms a generalized beamformer with multiple beams formed by orthogonal eigenvectors of the correlation matrix of the estimated channel at BS from uplink pilot sequences. This can be viewed as a form of feedback as well.

STBC transmissions demand instantaneous CSI at the receiver side to coherently decode the code word, sending DL pilots from BS to estimation channel at UEs. In a massive MIMO downlink where the BS (transmitter) has a large number of antennas, too many time-frequency resources would have to be spent on the pilots, hence lowering the net spectral efficiency to a greater extent.

3.4 DESIGNING INTEGRATED STBC PRECODER

To capitalize Spatial diversity gain and beam-forming gain precoder design starts with acquiring the strongest directions, in other words modeling the beam-former. $\mathbf{W} \in \mathbb{C}^{M \times diversityorder}$ consists of a number of vectors representing the diversity order. Space-Time Coding matrix, $\mathbf{S} \in \mathbb{C}^{diversityorder \times T}$, where T represents number of time symbols required, Orthogonal Space-Time Block Code (OSTBC) matrix of the diversity of order 4 can be modelled as (3.15) [32]. Downlink signal can be modeled as (3.16), where $\mathbf{w}_i^H \mathbf{h}_1$ is known as effective channel. As previously mentioned, (refer to section)
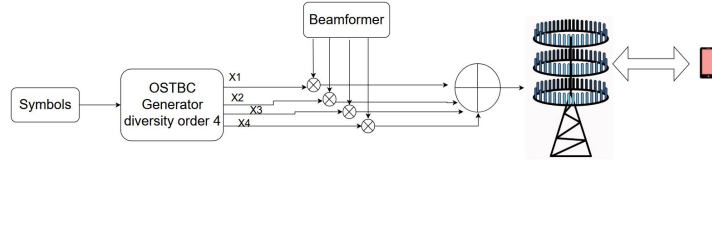
Figure 3.4: Single User System Model for Integrated STBC precoder.

instantaneous channel **h** with a huge dimension of M is required, BS has to transmit a pilot sequence of length as long as M, which further increases pilot overhead and reduction of spectral efficiency. By multiplying $\mathbf{W} \in \mathbb{C}^{M \times diversityorder}$ precoding with $\mathbf{S} \in \mathbb{C}^{diversityorder \times T}$ (each columns are orthogonal to each other), results in effective channel $\mathbf{W}^H\mathbf{h}$. Thus reducing the pilot over head from M to diversity order, the more diversity to be exploited results in more pilot symbols to be sent, to coherently decode the symbol with Maximum Likelihood Decoder.

$$\mathbf{S} = \begin{bmatrix} x_1 & -x_2 & -x_3 & -x_4 & x_1^* & -x_2^* & -x_3^* & -x_4^* \\ x_2 & x_1 & x_4 & -x_3 & x_2^* & x_1^* & x_4^* & -x_3^* \\ x_3 & -x_4 & x_1 & x_2 & x_3^* & -x_4^* & x_1^* & x_2^* \\ x_4 & x_3 & -x_2 & x_1 & x_4^* & x_3^* & -x_2^* & x_1^* \end{bmatrix} \tag{3.15}$$

$$\begin{bmatrix} y_1 & y_2 & \dots & y_T \end{bmatrix} = \mathbf{h}^H \begin{bmatrix} \mathbf{w}_1 & \mathbf{w}_2 & \mathbf{w}_3 & \mathbf{w}_4 \end{bmatrix} \mathbf{S} + noise \tag{3.16}$$
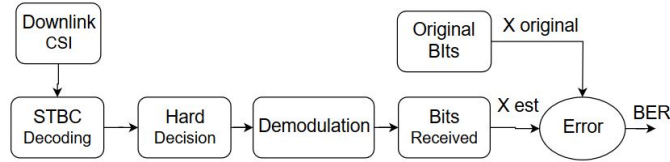
Figure 3.5: Block Diagram representing decoder for Beamforming and STBC precoder.

Figure 3.5 represents the decoder to calculate BER, STBC decoder uses downlink channel state information to coherently combine received symbols, which is followed by hard decider to map the decoded symbols using minimum Euclidean distance with the help of original constellation diagram.

3.4.1 Modelling simulated environment

To epitomize the closest real time scenario, we analyze the performance of Square pattern cells, with each cell area ($0.25km \times 0.25km$). The simulation parameters are listed in Table (3.1) .

Figure 3.6, corresponds to the performance of Integrated STBC precoder, exploiting both spatial diversity and Beam-Forming shows significant improvement in the performance of the system. But this new integrated Beam-Forming and STBC operate at rate 1/2, even though the higher reliability is observed this is not spectral efficient.

Table 3.1: System parameters chosen for Simulations

Index	Parameter	Value
1	M_{Tx}(No.of BS antennas)	128
2	N(No.of UE antennas)	1
3	K(No.of Users/cell)	4
4	Pathloss exponent	$\alpha = 3.76$
5	Shadow fading	$\sigma = 10$
6	Bandwidth	B = 20 MHz
7	Coherence Block	$\tau_p = 200$
8	OSTBC spatial diversity	Div.order = 4
9	Data Frame length	128
10	Modulation	QPSK
11	Number of cells	$L = [1\ 2]$
12	Pilot reuse	$f = 1$
13	Channel Model	One-Ring
14	Multipath Components	Q = 32
15	Angular Standard Deviation	$10°$
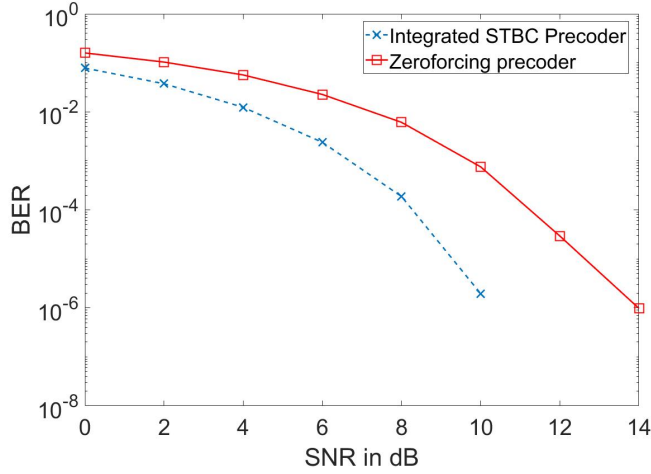
Figure 3.6: Performance of Integrated STBC precoder for a Single User scenario.

Every BS has to accommodate multiple active users, extending the derived precoder to provide services to multiple users, Figure 3.7 exposed the incapacity to suppress the inter-user interference.

3.4.2 Multi User precoder

Considering each user has Q multipath components channel matrix per each user, $\mathbf{H}_k \in \mathbb{C}^{Q \times M}$ can be modeled as:

$$\mathbf{H}_k = \begin{bmatrix} h_{1,1} & ... & h_{1,M} \\ . & . & . & . \\ . & . & . & . \\ h_{Q,1} & ... & h_{Q,M} \end{bmatrix} \tag{3.17}$$

Equivalent channel response per user $\mathbf{h}_k \in \mathbb{C}^{1 \times M}$ is expressed as sum of all Q multipath components.
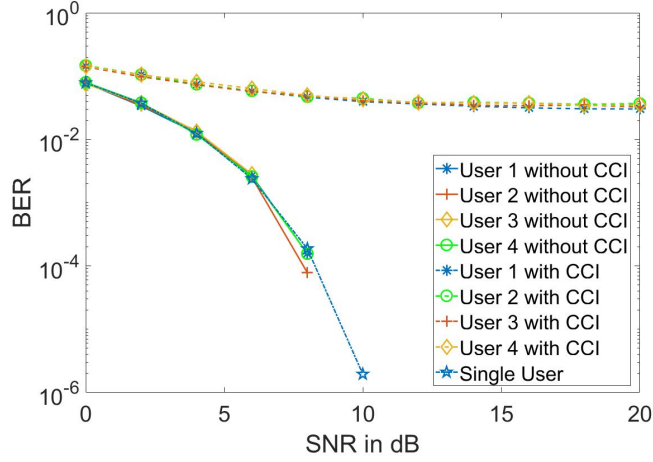
Figure 3.7: Comparison of Integrated STBC precoder for a Single User scenario vs Multi user scenario. (CCI means Inter-User Interference)

For every k-th user there are $K-1$ users to contributes inter-user interference, to precancel the interference at transmitter by forming interference channel matrix $\bar{\mathbf{H}}_{\mathbf{k}} \in \mathbb{C}^{M \times (K-1)}$ (3.18), should satisfy (3.19).

$$\bar{\mathbf{H}}_k = \begin{bmatrix} \mathbf{h}_1^H & ... & \mathbf{h}_{k-1}^H & \mathbf{h}_{k+1}^H & ... & \mathbf{h}_K^H \end{bmatrix} \tag{3.18}$$

$$\bar{\mathbf{H}}_k^H \mathbf{W}_k = 0 \tag{3.19}$$

One of the solutions to satisfy this condition is finding null subspace (3.20),

$$\mathbf{W}_k = \left(\mathbf{I} - \bar{\mathbf{H}}_k^\dagger \bar{\mathbf{H}}_k \right) \mathbf{D}_k, \prime \dagger\prime psuedoinverse \tag{3.20}$$

where $\mathbf{D}_k$ is an arbitary unitary matrix. In order to exploit the beamforming gain strongest directions can be found by performing SVD of (3.21) considering the corresponding strongest singular vectors to form arbitrary matrix $\mathbf{D}_k \in (M \times diversity\ order)$ [33].

$$\mathbf{G}_k = \mathbf{H}_k (\mathbf{I} - \bar{\mathbf{H}}_k^\dagger \bar{\mathbf{H}}_k) \tag{3.21}$$

As we considered a diversity order of 4, four strongest singular vectors corresponding to the four largest singular values used to construct the matrix $\mathbf{D}_k$.

Figure 3.8 shows that with perfect CSI at the BS and completely eliminating the interference performance is comparable to single user scenario. CSI plays a major role in the overall performance of the system. Gaining accurate CSI is very unlikely in real time scenarios, so robustness of the precoder should be analyzed under imperfect CSI.

Figure 3.9 gives the analysis of the imperfect channel knowledge. It is evident that good knowledge at transmitter plays a major role in successfully eliminating interference, even though precoder resulted in reduction of pilot overhead Downlink pilots are still required to coherently decode the symbols. In the next section we analysed how frequently CSI at the receiver should be updated.
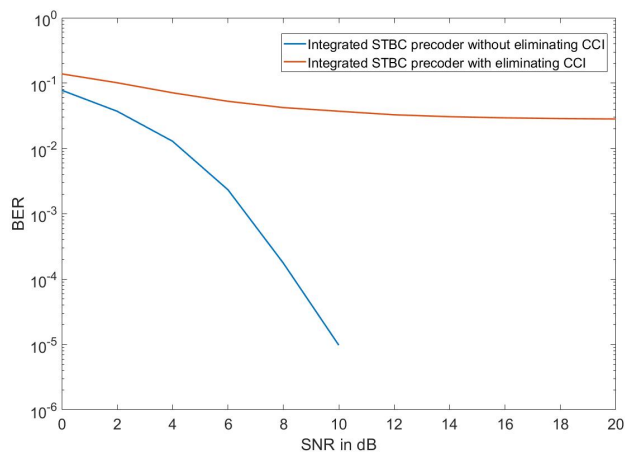
Figure 3.8: Performance of Integrated STBC precoder for a Multi user scenario with and without eliminating interference.
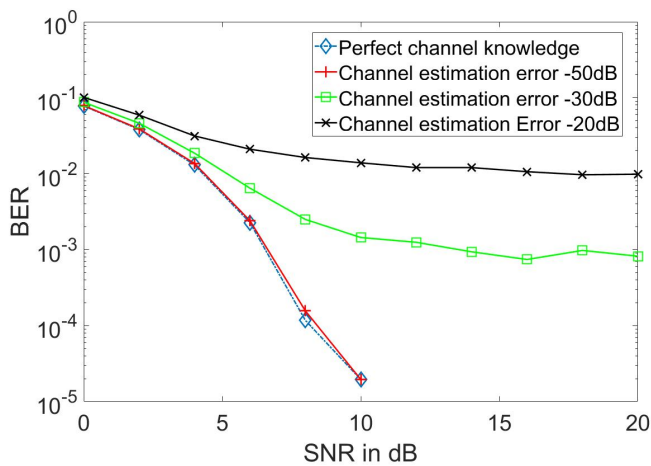
Figure 3.9: Performance of Integrated STBC precoder over imperfect channel knowledge.

3.5   COHERENCE TIME ANALYSIS OF THE PRECODER:

Considering an example of a cellular network with 128 transmitting antennas operating on LTE frame structure with 1200 subcarriers and 8 users, BS has to estimate approximately 1.3 million channel coefficients. As user increases the mobility the coherence block shrinks so the frequency of channel estimations increases, if frequency increases by x times then number of coefficients to be estimated also increases by a factor of x. As devised integrated precoders requires CSI to coherently combine and decode symbols at receiver, even though devised integrated precoder reduces the pilot over head but still channel estimation increases computational demand at receivers which indeed increases latency as well. In order to calculate how frequently receiver needs to estimate the channel coefficients, we considered the similar scenario considered in Section 2.5 which explained how quickly channel decorrelate.

To quantify the performance of the integrated STBC precoder under these dynamic real time channels, similar experiment set up as single user scenario (refer Figure 2.5) is considered. To assess the frequency at which CSI has to be updated of the devised integrated precoder (at SNR 10 dB) BER performance is analysed over different coherence blocks, assuming BS has CSI at every coherence block and the receiver has perfect channel information only at $t = 0$.
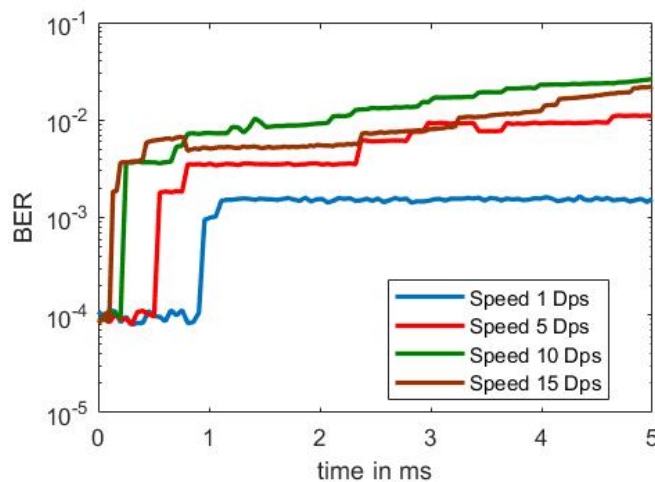
Figure 3.10: Performance analysis of Integrated STBC precoder for varying speeds.

Figure 3.10 results in following observations:

- User moving radially with a speed of 1Dps experience slower degradation in performance and it is evident that performance is constant in 1ms duration.

- As user started moving with higher speeds the more quicker degradation in performance is observed, for example user with 5 Dps experience constant performance till 0.5ms, as user reaches higher speeds this duration decreases.

- This demands more quicker CSI update at receiver, which demands downlink pilots which demands more resources.

3.6 SUMMARY:

This chapter outlined various diversity techniques and Space-Time Block Codes. Then we swiftly moved towards analyzing the inherent diversity introduced by deploying multiple antennas at the BS, and Diversity and Multiplexing tradeoff for linear precoders are analyzed. It has been observed that as multiplexing gain increased overall diversity gain offered by Massive MIMO systems is reduced, for Regular Zero-Forcing precoder the overall diversity gain is zero if multiplexing gain is introduced. Motivated by this, we explored integrating beamforming and STBC into massive MIMO to improve reliability. This new precoder achieved higher reliability at the cost of spectral efficiency. As, our main aim is to focus on eliminating the need for CSI at the receiver, so we limited our research not exploring various efficient techniques to improve the rate.

Integrated Beamforming and STBC precoder highly depend on channel knowledge at BS without accurate CSI inter-user interference are not properly mitigated, and the user cannot coherently combine and detect the symbols without accurate CSI. A radially moving scenario is modeled to analyze how frequently the user has to update it's CSI to maintain certain reliability. It has been observed that the quicker the user started moving the quicker the coherence block started shrinking. This increases the frequency of updating downlink CSI, further increasing the downlink pilot overhead. This motivated us in investigating new precoders to exploit the full spatial diversity, by eliminating the need for CSI at the user.

4 | SPACE-TIME LINE CODES: MASSIVE MIMO

As it is well established that STBC(Space Time Block Codes) allows us to gain full spatial diversity, but it comes with a shortcoming of having channel knowledge at the receiver to successfully decode the symbols. This necessity of requiring channel knowledge is demanding more resources. Section 3.5 showed that this is a quite expensive process and hindering the performance. [9] Proposed a novel rate one full spatial diversity technique, with 1 transmitting antenna and 2 receiving antennas and a blind combining scheme to decode. The sole requirement of CSI at transmitter alone and still able to exploit the full spatial diversity makes this technology more suitable in the current day communication systems, upsurge in low cost, low power, and low complexity demands such solutions.

4.1 SPACE TIME LINE CODE: INTRODUCTION

Figure 4.1 represents the classic STLC system with one transmitting antenna and two receiving antennas, with two independent channel gains h_1 and h_2 with CSI at the transmitter.
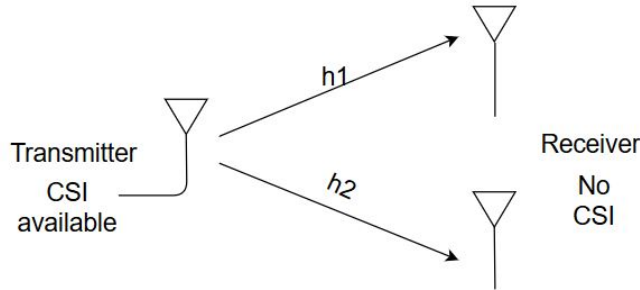
Figure 4.1: Block diagram of STLC.

4.1.1 Encoding and Decoding Scheme

STLC symbols s_1 and s_2 are encoded using information symbols x_1 and x_2 mathematically modelled as [9] :.

$$\begin{bmatrix} s_1^* \\ s_2 \end{bmatrix} = \begin{bmatrix} h_1 & h_2 \\ h_2^* & -h_1^* \end{bmatrix} \begin{bmatrix} x_1^* \\ x_2 \end{bmatrix} \tag{4.1}$$

Similar to STBC, two consecutive time slots are used to transmit s_1 and s_2 as expressed in (4.2). Transmitting two STLC symbols over two consecutive

symbols results in four symbols at receiver (4.3), where $\gamma_2 = |h_1|^2 + |h_2|^2$ represents *effective channel gain* to satisfy the transmit power constraint σ_x^2.

$$
\begin{aligned}
s_1 &= h_1^* x_1 + h_2^* x_2^* \\
s_2 &= h_2^* x_1^* - h_1^* x_2
\end{aligned}
\tag{4.2}
$$

$$
\begin{bmatrix} r_{1,1} & r_{1,2} \\ r_{2,1} & r_{2,2} \end{bmatrix} = \frac{1}{\sqrt{\gamma_2}} \begin{bmatrix} h_1 \\ h_2 \end{bmatrix} \underbrace{\begin{bmatrix} s_1 & s_2 \end{bmatrix}}_{STLCsymbols} + \begin{bmatrix} z_{1,1} & z_{1,2} \\ z_{2,1} & z_{2,2} \end{bmatrix}
\tag{4.3}
$$

To successfully separate x_1 and x_2 from the received four symbols and to still achieve full-spatial diversity a *blind-combining* technique (4.4) is used (see figure). Apart from achieving full spatial diversity as STBC demands full channel information and six operations of complex values. In contrast STLC decoding only requires two addition operations thus reducing the complexity by 75% [9].

$$
\begin{aligned}
r_{1,1} + r_{2,2}^* &= \sqrt{\gamma_2} x_1 + z_{1,1} + z_{2,2}^* \\
r_{2,1}^* - r_{1,2} &= \sqrt{\gamma_2} x_2 - z_{1,2} + z_{2,1}^*
\end{aligned}
\tag{4.4}
$$

Comparing the performance (see Figure 4.2) of STBC and STLC schemes it is very clear that both can achieve full-spatial diversity. Thus, replacing STBC with STLC is a well mixture of achieving diversity along with reduced complexity.
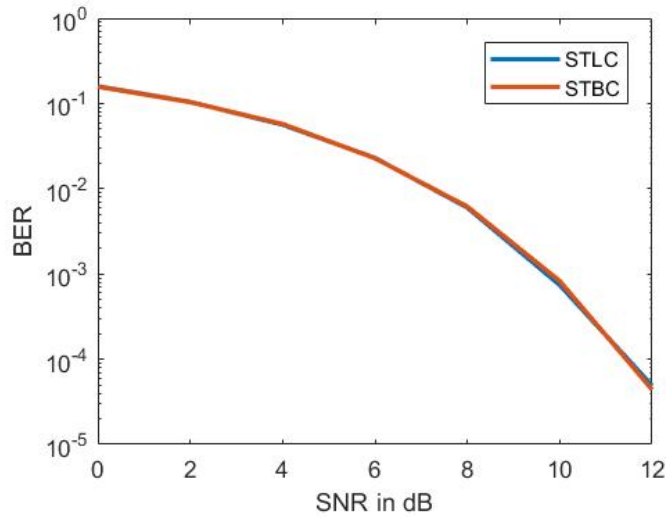
Figure 4.2: Performance comparison of STBC vs STLC.

4.2 SPACE TIME LINE CODES FOR MASSIVE MIMO

It is well established that Massive MIMO systems have their own distinctive properties, which grabbed huge attention and even considered to be an important technique in future cellular networks. Space diversity has its own perks and it is observed that there is a considerable advantage in adapting

STBC into the Massive MIMO scenario. Section 2.5 showed the neediness of having accurate CSI at the receiver, which turned out to be expensive. Now, new STLC encoding provided a proper solution in solving this shortcoming.

4.2.1 Encoding and Decoding process

Extending the 1×2 discussed to Massive MIMO scenario, system model should be upgraded to $M \times 2$. Consider $h_{n,m}$ the channel gain from m-th transmitting antenna to n-th receiving antenna, where $m \in \mathcal{M} = \{1, 2, ..., M\}$ and $n \in \{1, 2\}$. This section first explores the optimal STLC transmission scheme for a single user scenario and then extend to multi user and multi cell scenarios. Following the similar strategy to devise two space-time symbols to transmit in two consecutive time slots, $s_{m,1}$ and $s_{m,2}$, for each antenna, are modelled using information symbols x_1 and x_2 as follows (4.5) [34]:

$$
\begin{aligned}
s_{m,1} &= h_{1,m}^* x_1 + h_{2,m}^* x_2^* \\
s_{m,2} &= h_{2,m}^* x_1^* - h_{1,m}^* x_2
\end{aligned}
\tag{4.5}
$$

Normalizing factor $\eta = 1/\sqrt{\gamma_M}$ is introduced to keep the constant transmit power constraint σ_x^2, where γ_M effective channel gain represented as 4.6, such that $\sum_{m=1}^{M} \mathbf{E} |\eta s_{m,t}|^2 = \sigma_x^2$.

$$
\gamma_M = \sum_{m=1}^{M} |h_{1,m}|^2 + |h_{2,m}|^2
\tag{4.6}
$$

At the receiver coherently combing all the M transmitted symbols received in two consecutive time slots results in the following four symbols (4.7), where $z_{n,t}$ represents AWGN with zero mean and variance σ_z^2:

$$
r_{1,1} = \frac{1}{\sqrt{\gamma_M}} \left(\sum_{m=1}^{M} h_{1,m} s_{m,1} \right) + z_{1,1}
\tag{4.7}
$$

$$
r_{1,2} = \frac{1}{\sqrt{\gamma_M}} \left(\sum_{m=1}^{M} h_{1,m} s_{m,2} \right) + z_{1,2}
\tag{4.8}
$$

$$
r_{2,1} = \frac{1}{\sqrt{\gamma_M}} \left(\sum_{m=1}^{M} h_{2,m} s_{m,1} \right) + z_{2,1}
\tag{4.9}
$$

$$
r_{2,2} = \frac{1}{\sqrt{\gamma_M}} \left(\sum_{m=1}^{M} h_{2,m} s_{m,2} \right) + z_{2,2}
\tag{4.10}
$$

Without compromising the unique property of low complexity, *blind-combining* technique (4.4) is used:

$$
r_{1,1} + r_{2,2}^* = \frac{1}{\sqrt{\gamma_M}} \sum_{m=1}^{M} \left(h_{1,m} s_{m,1} + h_{1,m}^* s_{m,1}^* \right) + z_{1,1} + z_{2,2}^*
\tag{4.11}
$$

$$
= \sqrt{\gamma_M} x_1 + z_{1,1} - z_{2,2}^*
\tag{4.12}
$$

$$
r_{2,1}^* - r_{1,2} = \frac{1}{\sqrt{\gamma_M}} \sum_{m=1}^{M} \left(h_{2,m}^* s_{m,1}^* - h_{1,m} s_{m,2} \right) + z_{2,1}^* - z_{1,2}
\tag{4.13}
$$

$$
= \sqrt{\gamma_M} x_2 + z_{2,1}^* - z_{1,2}
\tag{4.14}
$$

Analysing the computationally complexity STLC massive MIMO scenario involves $4M$ multiplications, $2M$ complex additions and decoding process involves two addition [34].
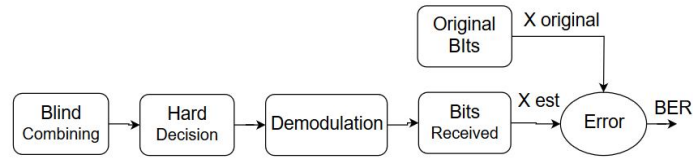
Figure 4.3: Block Digram representing decoder for STLC precoder.
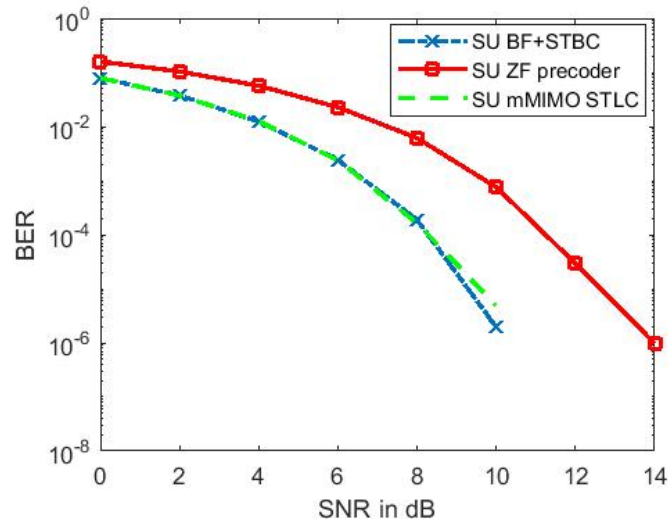
Figure 4.4: Performance comparison between mMIMO STLC precoder, Beamforming and STBC precoder and Zero forcing Precoder.

To analyse the performance of massive MIMO STLC precoder, an environment with the same characteristics modelled in Section 3.4.1 is used, Figure 4.3 represents the block diagram for the new STLC decoder. Figure 4.4 corresponds to the comparison of STLC precoder for massive MIMO system with Beamforming plus STBC precoder and Zero forcing precoder. It shows that STLC precoder achieves similar performance as Beamforming plus STBC precoder. Massive MIMO STLC precoder with rate 1 outclassed Zero-Forcing precoder as well as Beamforming plus STBC precoder, with rate 1/2. This further motivated us to analyze the robustness of the STLC precoder.

4.2.2 Channel Estimation Error Analysis:

As it is well established fact that it is very hard to gain the actual CSI, and due to limited orthogonal pilot sequences, pilot sequences are often repeated which further reduce the quality of channel state information. Integrated STBC precoder is highly depended on the quality of channel knowledge not only at the transmitter but at receiver as well. STLC precoder exhibited advantage of achieving full spatial diversity with blind combining

scheme without demanding any channel knowledge at the receiver. Assuming the uncertain channel model $\tilde{h}_n = h_n + \epsilon_n$, where $\epsilon_n \sim \mathbb{CN}(0, \sigma_\epsilon^2)$ results in following received symbols (4.15) :

$$r_{1,1} = \frac{1}{\sqrt{\gamma M}} \left(\sum_{m=1}^{M} h_{1,m} \tilde{s}_{m,1} \right) + z_{1,1} \tag{4.15}$$

$$r_{1,2} = \frac{1}{\sqrt{\gamma M}} \left(\sum_{m=1}^{M} h_{1,m} \tilde{s}_{m,2} \right) + z_{1,2} \tag{4.16}$$

$$r_{2,1} = \frac{1}{\sqrt{\gamma M}} \left(\sum_{m=1}^{M} h_{2,m} \tilde{s}_{m,1} \right) + z_{2,1} \tag{4.17}$$

$$r_{2,2} = \frac{1}{\sqrt{\gamma M}} \left(\sum_{m=1}^{M} h_{2,m} \tilde{s}_{m,2} \right) + z_{2,2} \tag{4.18}$$

where $\tilde{s}_{m,1}$ and $\tilde{s}_{m,1}$ represents encoded symbols with uncertain knowledge.

$$\tilde{s}_{m,1} = \frac{1}{\sqrt{\tilde{\gamma}_M}} \left(\tilde{h}_1^* x_1 + \tilde{h}_2^* x_2^* \right) \tag{4.19}$$

$$\tilde{s_{m,2}} = \frac{1}{\sqrt{\tilde{\gamma}_M}} \left(\tilde{h}_2^* x_1^* + \tilde{h}_1^* x_2 \right) \tag{4.20}$$

$$
\begin{aligned}
r_{1,1} + r_{2,2}^* &= \frac{\gamma_M}{\sqrt{\tilde{\gamma}_M}} x_1 + \frac{(h_1 \epsilon_1^* - h_2^* \epsilon_2) x_1}{\sqrt{\tilde{\gamma}_M}} \\
&+ \frac{(h_1 \epsilon_2^* + h_2^* \epsilon_1) x_2^*}{\sqrt{\tilde{\gamma}_M}} + z_{1,1} - z_{2,2}^* \\
r_{2,1}^* - r_{1,2}^* &= \frac{\gamma_M}{\sqrt{\tilde{\gamma}_M}} x_2 + \frac{(h_1 \epsilon_1^* + h_2^* \epsilon_2) x_2}{\sqrt{\tilde{\gamma}_M}} \\
&+ \frac{(h_2^* \epsilon_1 - h_1 \epsilon_2^*) x_1^*}{\sqrt{\tilde{\gamma}_M}} + z_{2,1}^* - z_{1,2}
\end{aligned}
\tag{4.21}
$$
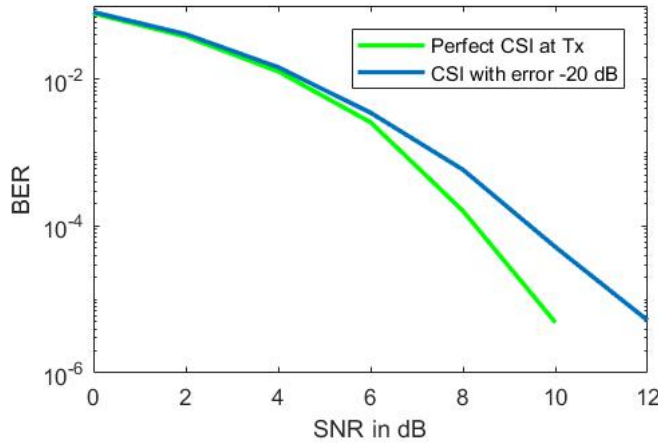
Figure 4.5: Performance analysis of STLC precoder for Single User scenario under imperfect CSI.

Figure 4.5 shows the performance of single user scenario under imperfect channel knowledge. It is observed that even with uncertainty, better performance is obtained.

4.3 MULTI USER STLC FOR MASSIVE MIMO

Accommodating multiple users is a must and introduces various levels of challenges to successfully provide service to each user with certain quality of performance. Considering M transmitting antennas, two receiving antennas and K users, where $k \in \{1,...K\}$, [34] proposed an antenna allocation scheme to shelter multiple users. This section outlines the analysis of the shortcomings of available antenna allocation schemes. Encoding and decoding schemes follow a similar pattern as previously discussed, where $m \in \mathcal{M}_k$, STLC symbols $s_{m,1}$ and $s_{m,2}$ are modelled using information symbols $x_{1,k}$ and $x_{2,k}$ for k-th user and $h_{n,k,m}$ represents channel coefficient of m-th transmit antenna to n-th receive antenna of k-th user.

$$\begin{bmatrix} s^*_{m,k,1} \\ s_{m,k,2} \end{bmatrix} = \begin{bmatrix} h_{1,k,m} & h_{2,k,m} \\ h^*_{2,k,m} & -h^*_{1,k,m} \end{bmatrix} \begin{bmatrix} x^*_{1,k} \\ x_{2,k} \end{bmatrix} \tag{4.22}$$

Effective channel gain for each user is reduced from γ_M to $\gamma_k = \sum_{m \in \mathcal{M}_k} |h_{1,k,m}|^2 + |h_{2,k,m}|^2$, but there is a first hand disadvantage of reduction of serving antennas, as discussed in [mMIMO 2.0] any system $<$ 64 transmitting antennas and not serving multiple users cannot be classified as Massive MIMO system. Apart from this, allocating antennas to different users contributes a huge interference from other antennas allocated for other users. Figure 4.6 shows that there is a huge interference contribution from other interfering antennas allocated from interfering user set $\mathcal{M}_{\bar{k}} = \mathcal{M}/\mathcal{M}_k$

4.3.1 SINR analysis

(4.11) represents the blind combining scheme and results in (4.23), even though antenna allocation provides a scheme to accommodate multiple users schematically Figure 4.6 shows that there is a huge interference from other users. This section focuses towards quantifying this inter antenna allocated interference.

$$SNR_{SU-STLC} = \frac{\gamma_M \sigma_x^2}{2\sigma_z^2} \tag{4.23}$$

Using the same *blind-combining*, received signal can be expressed as (4.24), where the second term represents the interference experienced by each user.

$$r_{n,t,k} = \frac{1}{\sqrt{\gamma_k}} \left(\sum_{m \in \mathcal{M}_k} h_{n,k,m} s_{m,t} \right)$$

$$+ \sum_{\bar{k} \in \mathcal{M}_{\bar{k}}} \left(\frac{1}{\sqrt{\gamma_{k'}}} \sum_{m' \in \mathcal{M}_{\bar{k}}} h_{n,k',m'} s_{m',t} \right) + z_{n,t,k} \tag{4.24}$$

$$r_{1,1,k} + r^*_{2,2,k} = \sqrt{\gamma_k} x_{1,k} + v_{1,k} + z_{1,1,k} + z^*_{2,2,k}$$
$$r^*_{2,1,k} - r_{1,2,k} = \sqrt{\gamma_k} x_{2,k} + v_{2,k} + z^*_{2,1,k} - z_{1,2,k} \tag{4.25}$$
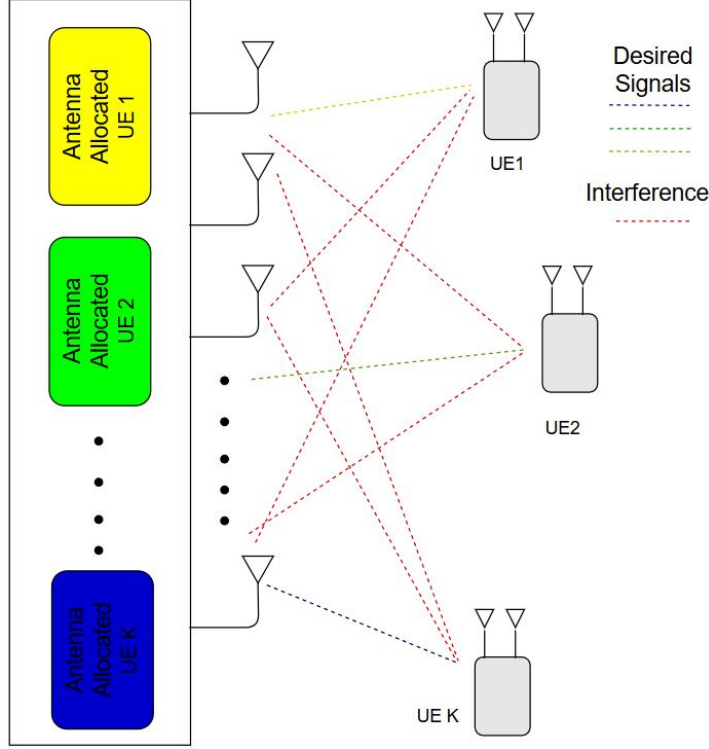
Figure 4.6: mMIMO system model for antenna allocation scheme for MU-STLC.

$$
\begin{aligned}
v_{1,\bar{k},m'} &= \begin{bmatrix} h_{1,k,m'} & h_{2,k,m'}^* \end{bmatrix} \begin{bmatrix} h_{1,\bar{k},m'}^* & -h_{2,\bar{k},m'}^* \\ h_{2,\bar{k},m'} & h_{1,\bar{k},m'} \end{bmatrix} \begin{bmatrix} x_{1,\bar{k}} \\ x_{2,\bar{k}}^* \end{bmatrix} \\
v_{2,\bar{k},m'} &= \begin{bmatrix} h_{1,k,m'} & h_{2,k,m'}^* \end{bmatrix} \begin{bmatrix} h_{2,\bar{k},m'}^* & h_{1,\bar{k},m'}^* \\ -h_{1,\bar{k},m'}^* & h_{2,\bar{k},m'}^* \end{bmatrix} \begin{bmatrix} x_{1,\bar{k}}^* \\ x_{2,\bar{k}} \end{bmatrix}
\end{aligned}
\tag{4.26}
$$

In (4.25), the $v_{1,k}$ and $v_{2,k}$ terms represent the total interference with respect to $x_{1,k}$ and $x_{2,k}$. This results in a received SINR of k-th user as (4.27), where σ_x^2, σ_z^2 and σ_v^2 corresponds to transmit power, noise power and interference. Even though this antenna allocation achieves full spatial diversity, inability to mitigate interference worsens the performance.

$$
SNR_{STLC} = \frac{\gamma_k \sigma_x^2}{2\sigma_z^2 + \sigma_v^2}
\tag{4.27}
$$

4.3.2 Antenna Allocation Schemes:

- User domain Greedy

- Antenna domain Greedy

USER-DOMAIN GREEDY

Allocation strategy is performed for each specific user to achieve the specific target SINR, and then is performed for another user. Allocating the best transmit antenna for each specific user maximizes SINR. The user selection is done based on channel quality based (CQB) approach. These allocation strategies result in allocating in S-antennas per each user.

ANTENNA-DOMAIN GREEDY

Antenna allocation strategy considers each user and allocating S antennas per user based on channel quality. S antennas are selected for each user based on the effective channel gain, and repeated for all users. Algorithm 4.1 represents the algorithm proposed for antenna greedy[34].

Even though theoretically SINR is optimized using above mentioned greedy algorithms, antenna allocation is never a solution as each user cannot exploit full array gain. We analyzed the performance of the precoder under the same scenario modelled using parameters defined in Table 3.1. Figure 4.7 shows that overall performance of the system is not acceptable, as inter-user interference is not completely eliminated.

Algorithm 4.1: ANTENNA GREED ALGORITHM

Input: $\mathcal{M} = \{1, ..., M\}$, $\mathcal{K} = \{1, ..., K\}$, CSI **h** and S number of antennas per each user.

Output: $\mathcal{M}_k$: set of all antennas allocated for k-th user.

1 **for** $k = 1 : K$ **do**

2   find antenna that has strongest channel gain corresponding to k-th user, i.e. find $\max_{m \in \mathcal{M}} \left\| h_{k,m} \right\|^2$ and allocate corresponding m-th antenna to k-th user and add this to $\mathcal{M}_k$ antenna subset.

3   **for** $j = 1 : S$ **do**

4   Update antenna set by removing the allocated antenna , i.e. $\mathcal{M}_{update} = \mathcal{M} \setminus m - th$ antenna previously allocated. Find antenna that has strongest channel gain corresponding to k-th user on new updated set, i.e. find $\max_{m \in \mathcal{M}_{update}} \left\| h_{k,m} \right\|^2$ and update the antenna subset.

5   perform this for all users.
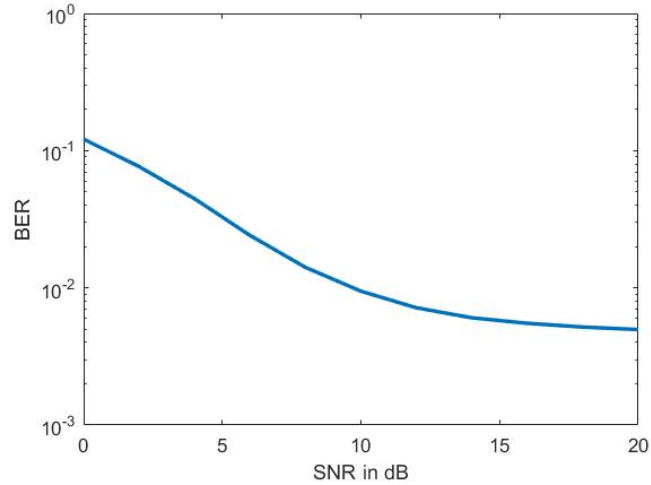
Figure 4.7: Performance analysis of MU STLC using Antenna Greedy allocation strategy.

4.4 PROPOSED INTEGRATED STLC PRECODER

Previous section evaluated effective SINR experienced for each user in (4.27) , and it is evident that antenna allocation schemes might reduce the interference but without proper suppression of interference the STLC precoder can never reach to its maximum potential. Without compromising the special characteristics: Low complexity and robustness against channel errors a seminal technique is proposed to eliminate the inter-symbol and inter-user interference, by integrating *ZF* coefficients into STLC precoder. As previously discussed antenna allocations schemes are not a proper solution because of inability to take the advantage of complete antenna array.

Observing the structure STLC symbols and receive combining schemes it is observed that inter-symbol interference is cancelled. It is evident that available antenna allocation schemes introduce extra interference terms. By observing *blind-combining* strategy in (4.11), it has been observed that :

$$
r_{1,1} + r_{2,2}^* = \frac{1}{\sqrt{\gamma_2}} \underbrace{(h_1 h_1^* + h_2^* h_2)\, x_1}_{Desired-Symbols} + \underbrace{(h_1 h_2^* - h_2^* h_1)\, x_2^*}_{Interfering-Symbols}
\tag{4.28}
$$

$$
r_{2,1}^* - r_{1,2} = \frac{1}{\sqrt{\gamma_2}} \underbrace{(h_2^* h_1 - h_1 h_2^*)\, x_1^*}_{Interfering-Symbols} + \underbrace{(h_2 h_2^* + h_1^* h_1)\, x_2}_{Desired-Symbols}
\tag{4.29}
$$

Analyzing (4.28) it is evident that symbols which are not meant for the desired antenna should be summed to zero. To suppress this inter-symbol interference new coefficients $w_{m,k}^r$ are introduced for each m-th transmitting antenna, r-th receiving antenna and k-th user, are adapted into Equation 4.30.

$$
\begin{bmatrix} s_{m,k,1}^* \\ s_{m,k,2} \end{bmatrix} = \begin{bmatrix} w_{m,k}^1 & w_{m,k}^2 \\ w_{m,k}^{2*} & -w_{m,k}^{1*} \end{bmatrix} \begin{bmatrix} x_{k,1}^* \\ x_{k,2} \end{bmatrix}
\tag{4.30}
$$

$$
\begin{aligned}
s_{m,k,1} &= (w_{m,k}^1)^* x_{k,1} + (w_{m,k}^2)^* x_{k,2} \\
s_{m,k,2} &= (w_{m,k}^2)^* x_{k,1}^* - w_{m,k}^2 x_{k,2}
\end{aligned}
\tag{4.31}
$$

First, we would like to develop a technique for a single user scenario, assuming $k = 1$, and extend this to a multi-user scenario. New STLC symbols can be represented as:

$$
\begin{aligned}
s_{m,1} &= (w_m^1)^* x_1 + (w_m^2)^* x_2 \\
s_{m,2} &= (w_m^2)^* x_1^* - w_m^2 x_2
\end{aligned}
\tag{4.32}
$$

Received symbols at m-th receiving antenna on t-th time slot can be represented as :

$$
r_{n,t} = \left(\sum_{m=1}^{M} h_{n,m} s_{m,t} \right) + z_{n,t}
\tag{4.33}
$$

Using the updated STLC, *blind-combining* can be represented as:

$$r_{1,1} + r_{2,2}^* = \underbrace{\sum_{m=1}^{M} \left(h_{1,m}(w_m^1)^* + h_{2,m}^* w_m^2 \right) x_1}_{Desired-Symbols}$$

$$+ \underbrace{\sum_{m=1}^{M} \left(h_{1,m}(w_m^2)^* - h_{2,m}^*(w_m^1)^* \right) x_2}_{Interfering-Symbols} + \underbrace{z_{1,1} + z_{2,2}^*}_{Noise} \quad (4.34)$$

$$r_{2,1}^* - r_{1,2} = \underbrace{\sum_{m=1}^{M} \left(h_{2,m}^*(w_m^1) - h_{1,m}(w_m^2)^* \right) x_1^*}_{Interfering-Symbols}$$

$$+ \underbrace{\sum_{m=1}^{M} \left(h_{2,m}^*(w_m^2) + h_{1,m}^*(w_m^1)^* \right) x_2}_{Desired-Symbols} + \underbrace{z_{2,1}^* - z_{1,2}}_{Noise} \quad (4.35)$$

In order to cancel the inter symbol interference, precoder should be satisfying following conditions :

$$\sum_{m=1}^{M} \left(h_{1,m}^*(w_m^1) \right) = \sum_{m=1}^{M} \left(h_{2,m}^*(w_m^2) \right) = 1 \quad (4.36)$$

$$\sum_{m=1}^{M} \left(h_{2,m}^*(w_m^1) \right) = \sum_{m=1}^{M} \left(h_{1,m}^*(w_m^2) \right) = 0 \quad (4.37)$$

Considering the channel matrix $\mathbf{H} \in \mathbb{C}^{M \times 2}$ and new precoder $\mathbf{W} \in \mathbb{C}^{M \times 2}$ with updated coefficients,above conditions can be loosely translated as:

$$\mathbf{W}^H \mathbf{H} = \mathbf{I}_2 \quad (4.38)$$

A simple solution for this is to calculate Zero-Forcing coefficients. Using Zero-Forcing coefficients would be perfect in this scenario considering the fact that it is computationally affordable.

$$\mathbf{W} = \mathbf{H} \left(\mathbf{H}^H \mathbf{H} + \sigma^2 \mathbf{I} \right)^{-1} \quad (4.39)$$

Where σ^2 is a regularization factor to avoid the poor channel inversions. We introduced a regularization factor of 10^{-12} in ZF precoder to make good channel inversions.

Respecting the fact that ZF precoder can decouple the multi-user channel into independent single-user channels, modeled integrated STLC can easily be adapted for multi-user scenarios. Extending our new precoder to accommodate multiple users introduce inter-user interference along with inter-symbol interference. Considering $\mathcal{U} = \{1, 2, ..., K\}$, set of K users to be accommodated, for every k-th user there exists $K - 1$ interfering users $\bar{\mathcal{U}} = \mathcal{U} \setminus \{k\}$
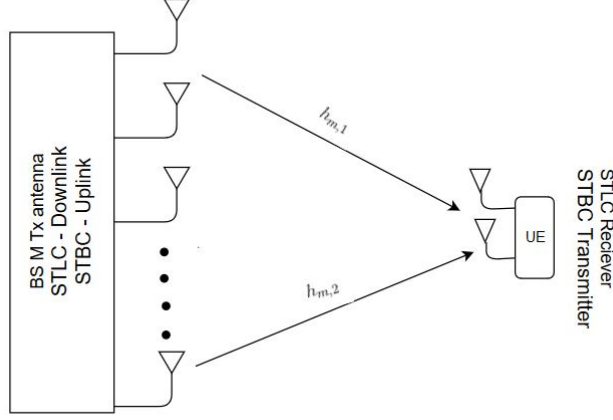
Figure 4.8: mMIMO system model for antenna allocation scheme for MU-STLC.

$$r_{n,t,k} = \underbrace{\left(\sum_{m=1}^{M} h_{n,k,m} s_{m,k,t} \right)}_{Desired-Symbols}$$

$$+ \sum_{\bar{k} \in \mathcal{U}} \underbrace{\left(\sum_{m=1}^{M} h_{n,k',m'} s_{m,\bar{k},t} \right)}_{Interuser-Interference} + \underbrace{z_{n,t,k}}_{Noise} \quad (4.40)$$

In (4.39), we have already discussed how to suppress the inter-symbol interference, let's focus on eliminating inter-user interference. BS obtains the channel matrix of $\mathbf{H} \in \mathbb{C}^{M \times 2K}$, where $\mathbf{H}_k \in \mathbb{C}^{M \times 2}$ represents the channel matrix of k-th user and $\bar{\mathbf{H}}_k \in \mathbb{C}^{M \times 2(K-1)}$ represents the channel interference matrix for k-th user, plugging the updated channel matrix into (4.39) a new integrated STLC precoder $\mathbf{W} \in \mathbb{C}^{M \times 2K}$ is derived. $\mathbf{W}_k \in \mathbb{C}^{M \times 2}$ two columns of the new integrated precoder $\mathbf{W}$ represents the new precoder coefficients for k-th user such that:

$$(\mathbf{W}_k)^H \mathbf{H}_k = \mathbf{I}_2 \tag{4.41}$$

$$(\mathbf{W}_k)^H \bar{\mathbf{H}}_k = \mathbf{0}_{(2 \times 2(K-1))} \tag{4.42}$$

With perfect CSI at BS obtained new precoder successfully eliminates the inter-symbol and inter-user interference.

Integrated STLC precoder has better performance, in the latter section, its resilience towards channel uncertainty is also analyzed. BS has M transmitting antennas along with CSI and UE has two transmitting antennas with no CSI, it is obvious that STLC achieves full spatial diversity, i.e $2M$. Up-link can also exploit the two transmitting antennas and achieve full spatial diversity using *alamouti* sequences or other space-time codes, as represented in Figure 4.8. Along with achieving extra spatial diversity from uplink-downlink pilot overhead and extra computational complexity at the receiver is avoided.

To verify the robustness of the proposed integrated STLC precoder, performance under uncertain CSI should be analyzed. To make a qualitative

analysis of the performance, the closest real-time scenario, 4 cells with pilot reuse factor 1, is epitomized, so that there is a possibility of having more uncertainty. Pilot contamination contributes towards a major hindrance in obtaining the actual channel knowledge.

Considering the imperfect channel knowledge $\tilde{H} \in \mathbb{C}^{M \times 2K}$, new precoder $\tilde{W}$ is devised:

$$\tilde{\mathbf{W}} = \tilde{\mathbf{H}} \left(\tilde{\mathbf{H}}^{H} \tilde{\mathbf{H}} + \sigma^2 \mathbf{I} \right)^{-1} \tag{4.43}$$
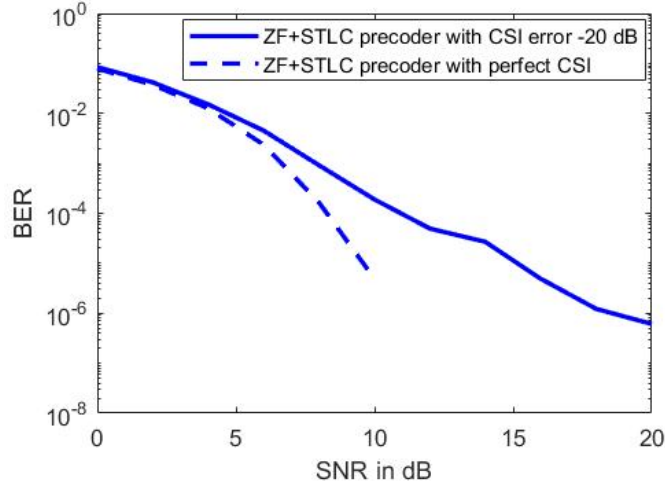
Figure 4.9: Performance analysis of integrated STLC precoder with pilot reuse factor 1 for K = 4.

Figure 4.9 outlines the comparison of Integrated STLC precoder, under perfect and imperfect CSI. It is evident that perfect CSI at BS is still required to reach the optimal performance, but performance under imperfect CSI is still acceptable. By assuming BS has the CSI (obtained using uplink pilot sequences) of each user in each cell under the pilot reuse factor of 1 proposed Integrated ZF STLC precoder showed resilience towards interference and error floor is observed as the number of users increases.

Having 2 antennas at receiver offers an added advantage to exploit diversity from uplink as well. This would not only improves of the overall system diversity, it would help us to improve the CSI as pilot sequences can also exploit the diversity through uplink. Exploiting STLC on downlink and STBC on uplink will improve the overall reliability of the system and reduce the demand of CSI at receiver, which will relax the complexity burden, which further decrease the overall end to end latency. Table 4.1 represents the overall system model:

Table 4.1: System model for Uplink and Downlink models

	No.of Antennas	Channel Knowledge	Downlink	Uplink
BS	M	CSI available	STLC enc.	STBC Rx.
UE	2	No CSI	Blind combining	STBC Tx.

In order to obtain the CSI, each user has to accommodate two pilot sequences, and pilot sequences are very limited resources. These pilot se-

quences play a major role in estimating the channels and they must be orthogonal. So these pilot sequences are reused among different cells, which will degrade the quality of channel estimated at BS. This is more severe in Massive MIMO compared to conventional communication systems, since it is supposed to accommodate more active terminals on the same time/frequency/spatial resources than conventional systems, the pilot contamination will be much severe in. Many studies have been explored to combat this *pilot-contamination*, as the main objective of the thesis not oriented towards this discussion, we limited our focus by not exploring any pilot decontamination techniques.

Accommodating two pilot sequences per user will further increase the scarcity of orthogonal pilot sequences, along with boosting the pilot contamination. As we are not focusing on pilot decontamination. An alternative technique is proposed to which can still achieve full spatial diversity with one receiver antenna.

4.5 ALTERNATIVE INTEGRATED STLC PRECODER

The previous section demonstrated that integrating a linear precoder and STLC leads to improvement in reliability and robustness towards channel uncertainty. Since orthogonal pilot sequences are limited and assigning two orthogonal sequences per each user is not an optimal strategy. Inspired by this problem statement a new novel STLC structure is proposed to achieve full spatial diversity with one receiving antenna.

To model this new precoder with a single receiving antenna, let's revisit the classical STLC system model (M Transmitting antennas and 2 Receiving antennas). Considering, $Q \in \mathbb{C}^{M \times 2}$ as new precoder, with $q_{m,1}$ and $q_{m,2}$ are new precoding coefficients for m-th transmitting antenna to form the following STLC symbols:

$$s_{m,1} = q_{m,1}^* x_1 + q_{m,2}^* x_2^* \tag{4.44}$$

$$s_{m,2} = q_{m,2}^* x_1^* - q_{m,1}^* x_2 \tag{4.45}$$

To make a better analysis of received symbols noise term and normalization factor is not considered, to obtain the following equations:

	Receiving Antenna-2	Receiving Antenna-2
t = 1	$\sum_{m=1}^{M}(h_{m,1}(q_{m,1}^* x_1 + q_{m,2}^* x_2^*))$	$\sum_{m=1}^{M}(h_{m,2}(q_{m,1}^* x_1 + q_{m,2}^* x_2^*))$
t = 2	$\sum_{m=1}^{M}(h_{m,1}(q_{m,2}^* x_1^* - q_{m,1}^* x_2))$	$\sum_{m=1}^{M}(h_{m,2}(q_{m,2}^* x_1^* - q_{m,1}^* x_2))$

Two receiving antennas allow identifying the symbols in two directions if we consider a single receiving antenna we are indeed eliminating one particular direction. The antenna array can be exploited to make two directions, M antenna system can be divided into two antenna array subsets, with $M/2$ antennas per each subset. Considering the obtained channel ma-

trix $\mathbf{h} \in \mathbb{C}^{M \times 1}$, $\mathbf{f}$ and $\mathbf{g}$ are modelled as (Figure 4.10 pictorial representation) :

$$
\mathbf{f} = \begin{bmatrix} h_1 \\ h_2 \\ . \\ . \\ h_{M/2} \end{bmatrix} \quad \mathbf{g} = \begin{bmatrix} h_{M/2+1} \\ h_{M/2+2} \\ . \\ . \\ h_M \end{bmatrix} \tag{4.46}
$$
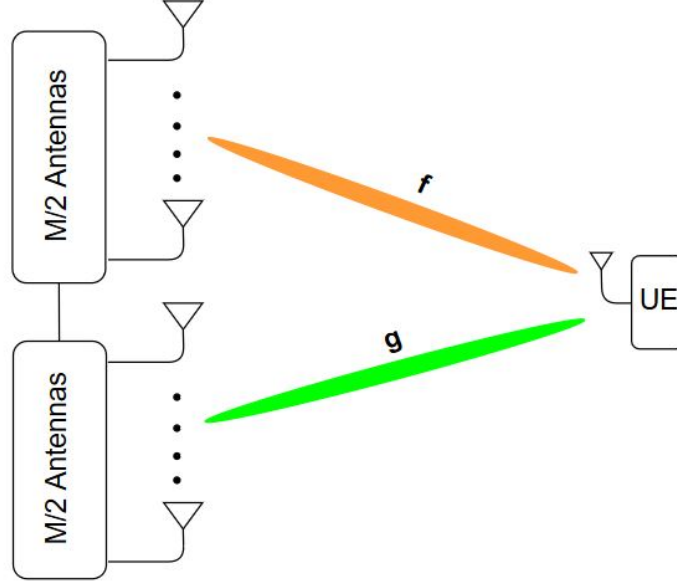
Figure 4.10: Alternative STLC precoder structure.

Receiver with single antenna coherently combines every signal it receives. This results in the following received symbols :

$$
r_1 = \left(\sum_{m=1}^{M} h_m \left(q_{m,1}^* x_1 + q_{m,2}^* x_2^* \right) \right) + z_1 \tag{4.47}
$$

$$
r_2 = \left(\sum_{m=1}^{M} h_m \left(q_{m,2}^* x_1^* - q_{m,1}^* x_2 \right) \right) + z_2 \tag{4.48}
$$

Which can be further written as:

$$
r_1 = \left(\sum_{m=1}^{M/2} f_m q_{m,1}^* + \sum_{m=1}^{M/2} g_m q_{m,1}^* \right) x_1 + \left(\sum_{m=1}^{M/2} f_m q_{m,2}^* + \sum_{m=1}^{M/2} g_m q_{m,2}^* \right) x_2^*
$$
$$
+ z_1 \tag{4.49}
$$

$$
r_2 = \left(\sum_{m=1}^{M/2} f_m q_{m,2}^* + \sum_{m=1}^{M/2} g_m q_{m,2}^* \right) x_1^* - \left(\sum_{m=1}^{M/2} f_m q_{m,1}^* + \sum_{m=1}^{M/2} g_m q_{m,1}^* \right) x_2
$$
$$
+ z_2 \tag{4.50}
$$

Following *blind-combining* strategy following symbols are retrieved:

$$r_1 + r_2^* = \sum_{m=1}^{M/2} \left(f_m q_{m,1}^* + g_m q_{m,1}^* + f_m^* q_{m,2} + g_m^* q_{m,2} \right) x_1$$

$$- \sum_{m=1}^{M/2} \left(f_m q_{m,2}^* + g_m q_{m,2}^* - f_m^* q_{m,1} - g_m^* q_{m,1} \right) x_2^* + z_1 + z_2^* \quad (4.51)$$

$$r_1^* - r_2 = \sum_{m=1}^{M/2} \left(f_m^* q_{m,1} + g_m^* q_{m,1} - f_m q_{m,2}^* - g_m q_{m,2}^* \right) x_1^*$$

$$+ \sum_{m=1}^{M/2} \left(f_m^* q_{m,2} + g_m^* q_{m,2} + f_m q_{m,1}^* + g_m q_{m,1}^* \right) x_2 + z_1^* - z_2 \quad (4.52)$$

In order to suppress the inter-symbol interference, this new STLC precoder should successfully separate the symbols received in two directions. Following conditions should be satisfied :

$$\begin{array}{rcl}
\sum_{m=1}^{M/2} f_m^* q_{m,1} = & \sum_{m=1}^{M/2} f_m q_{m,1}^* = & 1 \\
\sum_{m=1}^{M/2} f_m^* q_{m,2} = & \sum_{m=1}^{M/2} f_m q_{m,2}^* = & 0 \\
\sum_{m=1}^{M/2} g_m^* q_{m,1} = & \sum_{m=1}^{M/2} g_m q_{m,1}^* = & 0 \\
\sum_{m=1}^{M/2} g_m^* q_{m,2} = & \sum_{m=1}^{M/2} g_m q_{m,2}^* = & 1
\end{array} \quad (4.53)$$

One possible solution is to form new channel matrix $\mathbf{G}_{M/2 \times 2} = \begin{bmatrix} \mathbf{f} & \mathbf{g} \end{bmatrix}$ and calculating Zero-Forcing coefficients:

$$\mathbf{Q}_{temp} = \mathbf{G} \left(\mathbf{G}^H \mathbf{G} + \sigma^2 I \right)^{-1} \quad (4.54)$$

$\mathbf{Q}_{temp} \in \mathbb{C}^{M/2 \times 2}$ corresponds to Zero-Forcing coefficients, new integrated STLC precoder $\mathbf{Q} \in \mathbb{C}^{M \times 2}$ is formed by stacking the obtained Zero-Forcing coefficients together to completely use the full antenna array.

$$\mathbf{Q} = \begin{bmatrix} \mathbf{Q}_{temp} \\ \mathbf{Q}_{temp} \end{bmatrix} \quad (4.55)$$

Robustness of the new precoder under imperfect channel knowledge plays a major role, as gaining accurate channel information is very challenging, so it is important to analyze the performance of the system under imperfect CSI. New respective Zero-forcing coefficients $\tilde{\mathbf{Q}}_{temp}$, are calculated, by forming obtained channel knowledge $\tilde{\mathbf{F}}$.

$r_1 + r_2^*$ and $r_2^* - r_1$ can be used to decode x_1 and x_2 using respectively.

$$r_1 + r_2^* = \left(\mathbf{q}_1^H \mathbf{f} + \mathbf{q}_2^H \mathbf{g} \right) x_1 + z_1 + z_2^* \quad (4.56)$$

$$r_2^* - r_1 = \left(\mathbf{q}_2^H \mathbf{g} + \mathbf{q}_1^H \mathbf{f} \right) x_2 + z_1^* - z_2 \quad (4.57)$$

Equation (4.56) showed that this new approach results in the same performance as Massive MIMO STLC precoder. Simulating the new novel precoder under the same scenario Figure 4.12 showed that with perfect CSI both the alternative integrated STLC precoder showed similar performance
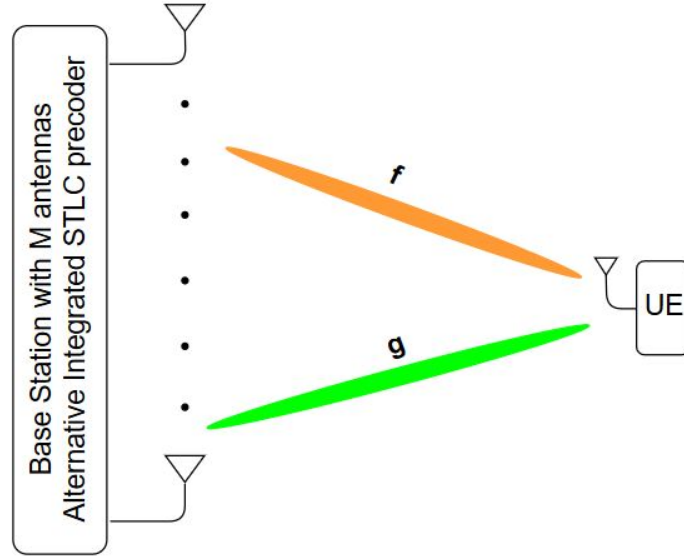
Figure 4.11: Alternative Integrated STLC encoding technique for Massive MIMO Scenario.

as integrated STLC precoder with two receiving antennas. So this new technique provided a new approach to achieve full spatial diversity with 1 receiving antenna. As previous section mentioned that having two receiving antennas increases the necessity of having two orthogonal pilots per each terminal, a new approach removed this necessity and makes this technique more promising. Along with achieving good performance it also exhibited similar resilience towards the channel uncertainty.

4.5.1 Multi-User Scenario:

Channel information, $\mathbf{H} \in \mathbb{C}^{M \times K}$, from all K users is acquired using uplink pilot sequences. Following the similar strategy shown in Figure 4.10, channel knowledge is divided into half which results in $\mathbf{F}_{MU} \in \mathbb{C}^{M/2 \times 2K}$, Zero-forcing precoder shown better performance in suppressing interference. New precoder, $\mathbf{Q}_{MU} \in \mathbb{C}^{M/2 \times 2K}$, is devised using Zero-Forcing technique:

$$\mathbf{Q}_{MU} = \mathbf{F}_{MU} \left(\mathbf{F}_{MU}{}^{H} \mathbf{F}_{MU} + \sigma^2 I \right)^{-1} \tag{4.58}$$

Figure 4.13 represents block diagram of alternative integrated STLC precoder for multi-user scenario, Figure 4.12 showed that alternative encoding technique is achieving the similar performance as integrated STLC precoder with 2 receiving antennas. When both precoders are tested under Multi-User scenarios with imperfect channel knowledge at transmitter, Figure 4.14 shows integrated STLC precoder with 2 receiving antennas exhibited better performance compare to alternative encoding technique for users with 1 receive antenna, but still this performance is comparable.

Integrated STLC precoder with two receiving antennas utilize four received symbols on two consecutive time slots to identify two desired symbols. This offers better protection compared to the systems with single antenna system where two symbols are received to detect two desired symbols.
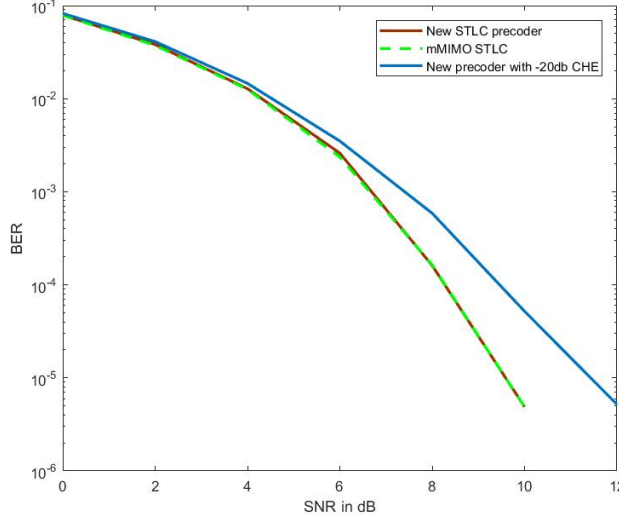
Figure 4.12: Performance analysis of new precoder compared.

4.6 COMPUTATIONALLY COMPLEXITY ANALYSIS:

STLC precoders showed that they could achieve full spatial diversity, with less computational demands. This has grabbed our attention to explore new novel technique to accommodate multiple users. In this section we analysed the computational complexity of proposed precoders for encoding and decoding. Exact complexity depends strongly on hardware implementation. Addition and subtraction operations are easier to implement in hardware, so complex multiplications and divisions are considered to estimate computational complexity. Following lemmas are used to calculate number of complex multiplications required [35,36]:

- **Lemma 1** Considering matrices $\mathbf{A} \in \mathbb{C}^{N_1 \times N_2}$ and $\mathbf{B} \in \mathbb{C}^{N_2 \times N_3}$, $\mathbf{AB}$ requires $N_1 N_2 N_3$ complex multiplications, where $\mathbf{AA}^H$ demands $\frac{N_1^2 + N_1}{2} N_2$ by utilizing Hermitian symmetry.

- **Lemma 2** Considering matrices $\mathbf{A} \in \mathbb{C}^{N_1 \times N_2}$ and $\mathbf{B} \in \mathbb{C}^{N_2 \times N_3}$, in order to compute $\mathbf{A}^{-1}\mathbf{B}$ $N_1^2 N_2$ complex multiplications are required, $\mathbf{LDL}^H$ decomposition can be used to efficiently to multiply inverse of a matrix by another matrix.

Massive MIMO STLC encoding requires $4M$ complex multiplications and $2M$ complex additions are required, while decoding requires only two complex additions are required. However, proposed new precoders for Multi-User scenario using ZF increase the computational complexity. We calculate the number of complex multiplications required for such precoders, while maintaining the same decoding complexity is targeted. Following Table 4.2 represents the complex multiplications required for precoders.

Observing Figure 4.16 and Figure 4.15, we can infer that Integrated STLC precoder and Alternative Integrated STLC precoder designed are having comparable computational complexity with Zero-Forcing precoder.
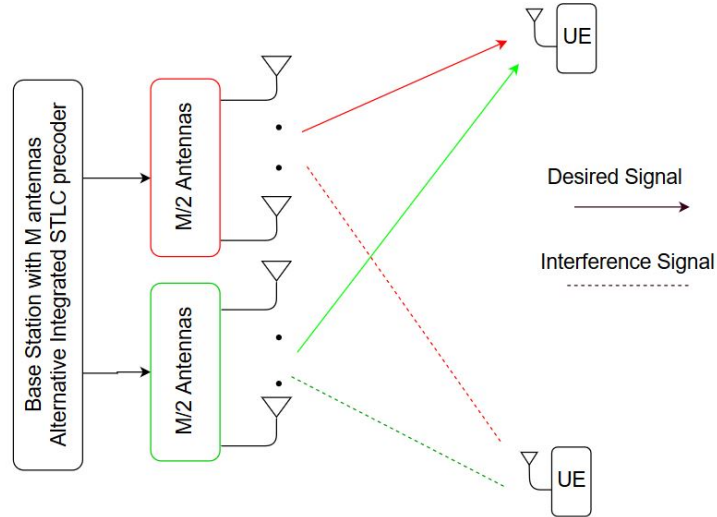
Figure 4.13: New STLC encoding technique for Multi-User Massive MIMO Scenario.
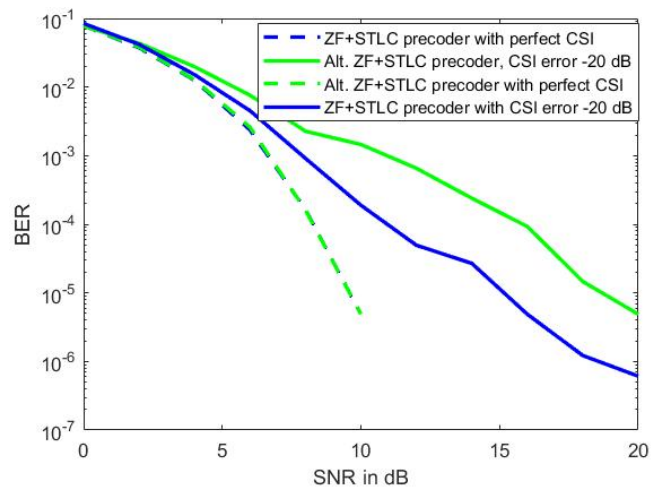
Figure 4.14: Performance analysis of Alternative integrated STLC precoder with pilot reuse factor 1 for K = 4 users.

4.7 SUMMARY:

This chapter outlined Space Time Line Codes and their advantage over Space Time Block Codes as the receiver doesn't demand any CSI to coherently decode the desired symbols. Inspired by computationally effective STLC system, the performance of STLC encoding strategy for Massive MIMO systems are analyzed and it has been observed that their performance is comparable with Beamforming combined STBC technique, with a better rate, we can say that STLC precoder for Massive MIMO has outclassed Beamforming combined STBC precoder. To accommodate multiple active users antenna allocation strategies are discussed, but these techniques are not optimal due to the inability to eliminate the inter-user interference.

Table 4.2: Computational Complexity Analysis.

Precoder	Comp. Multiplications
Zero forcing	$\frac{3K^2M}{2} + \frac{KM}{2} + \frac{K^3-K}{3}$
STLC-SU	$4M$
Integrated STLC precoder	$\frac{3K^2M}{2} + \frac{KM}{2} + \frac{K^3-K}{3} + 4M$
Alternative STLC precoder	$3K^2M + \frac{KM}{2} + \frac{8K^3-2K}{3} + 4M$
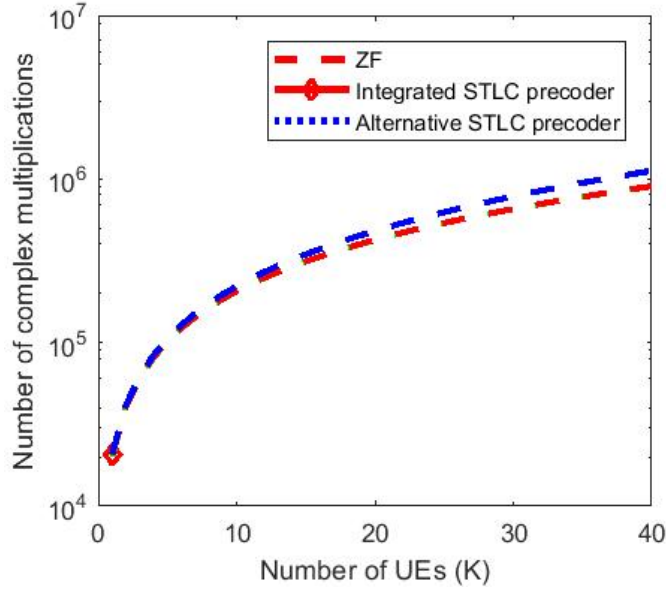
Figure 4.15: Number of complex multiplications required for varying K users and BS with $M = 128$ antennas
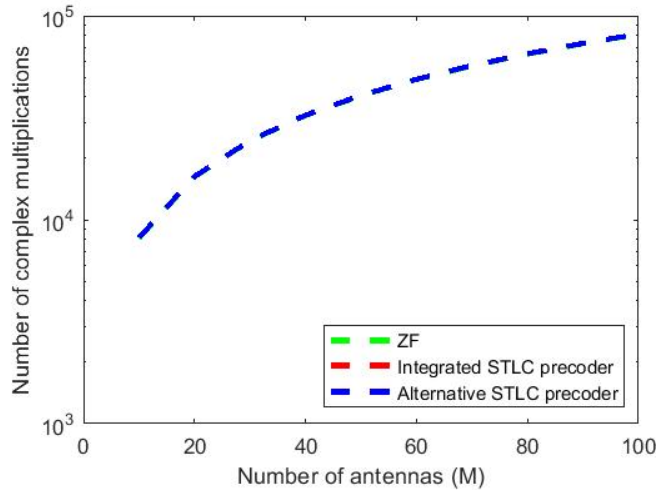
Figure 4.16: Number of complex multiplications required for varying M and for $K = 4$ users.

To address this issue a new integrated Zero-Forcing and STLC precoder is proposed, and it's robustness to eliminate inter-user and inter-symbol interference is analyzed under perfect CSI and imperfect CSI at the BS. Each

user with two antennas has to accommodate two uplink pilot sequences, as orthogonal pilot sequences are limited resources, results in indulging more frequent pilot reuse. This indeed triggers pilot-contamination, which makes it harder to gain accurate CSI at BS. As our system model depends on CSI at the receiver, pilot-contamination is a major instigator. To eliminate this need for extra pilot sequence per each user, another novel precoder is proposed to exploit full spatial diversity offered by STLC precoder with a single receiving antenna. With accurate channel knowledge at alternative integrated STLC precoder has shown indistinguishable performance with integrated Zero-Forcing precoder with two receiving antennas, but new precoder is not as robust as integrated Zero-Forcing and STLC precoder with two receiving antennas.

5 | CONCLUSIONS AND FUTURE PERSPECTIVES

This thesis investigated Space-time codes suitable for Massive MIMO systems, where both spatial multiplexing gain and spatial diversity gain can be exploited. Space-time codes gained a lot of attention because of their capabilities to achieve full spatial diversity. Space-time codes depend on the instantaneous channel or the statistical knowledge to coherently decode the symbols.

A brief introduction of Massive MIMO systems and the analysis of inherent diversity is discussed in Chapter 2 and Chapter 3. The diversity gain of the system depends on the multiplexing gain and quality of channel knowledge available at the transmitter and the receiver. Precoding techniques, like Zero-Forcing and Regular Zero-Forcing, gained wide popularity to support multiple users. The diversity and multiplexing gain trade-off of such precoding techniques is analyzed. Considering this as a motivation, integrating space-time block codes into Massive MIMO systems is explored. Section 3.3 provided a widely proposed technique to create multiple beams onto which branches of STBC symbols are superimposed and transmitted. Multiple beams are generated using eigenvalue decomposition of the correlation matrix. Precoder matrix devised $\mathbf{W} \in \mathbb{C}^{M \times diversity}$, results in effective channel vector $\mathbf{W}^H \mathbf{h} \in \mathbb{C}^{diversity \times 1}$ which reduced the overall pilot overhead. In a multi-user scenario interference channel matrix for each user is acquired, where the null subspace is derived to form orthogonal beams to superimpose corresponding STBC branches of the user. Gaining accurate channel knowledge is very difficult. The devised precoder is tested under imperfect knowledge conditions and it is observed that this precoder demands accurate channel information for better performance. Real-time wireless channels are very dynamic in nature, temporal channel analysis of a radially moving user is modelled to investigate how quickly channels becomes significantly different. This analysis showed that as the user's mobility increases coherence blocks started shrinking, which results in more frequent demand for downlink pilots. Considering this as a motivation, channel-independent decoding techniques to achieve full spatial diversity are explored.

Space-time-line-codes gained a lot of attention because of their simplified encoding and decoding structure. A classical STLC encoding structure has 1 transmit antenna and 2 receiving antennas, and it is observed that they have the same performance of classical STBC. STLC scheme is impressive because of its simplified encoding and decoding structure. We adapted the STLC encoding strategy into Massive MIMO scenario, and it is observed that a total spatial diversity of $2M$ is achieved. Accommodating multiple users is an integral part of cellular systems, we derived novel integrated STLC precoder with the help of Zero-Forcing precoder and it is observed that with accurate channel knowledge, we can achieve a 2dB gain in achieving a BER of 10^{-6}. Analyzing the integrated STLC precoder under inaccurate channel information showed greater resilience and better performance is observed compared to Beamforming and STBC precoder. But it has been observed that as each

user has 2 antennas BS has to accommodate 2 different pilot sequences to gain CSI at BS, this indeed is not a good strategy. So an alternative integrated STLC precoder using ZF precoder is derived to achieve full spatial diversity for users having a single transmit antenna. With perfect channel knowledge, it has been observed that alternative STLC structure has shown a similar performance and good perseverance towards imperfect channel knowledge at BS.

We have proposed two novel encoding strategies to gain full spatial diversity and it has been observed that proposed strategies resulted in achieving similar performance as beamforming and STBC with much lesser computational complexity and decoding process resulted in a reduction of 75 percent computational complexity.

5.1 FUTURE PERSPECTIVES:

This thesis has contributed new techniques to adapt space-time codes into massive MIMO systems. Research studies in this thesis lead to various interesting research interests. Here we provide some possible extensions to the proposed techniques.

- In this thesis, we have considered a single cell multi-user scenario. An analysis of the proposed integrated precoders under multi-cell scenarios and performance analysis under intra-cell interference could provide some interesting results.

- Proposed precoders simplified the decoding process, analysing the end to end latency by simulating real-time scenario situations corresponds to factory automation scenario. As URLLC services gained a lot of attention in providing tactile internet, vehicular communications, automation in factories, etc, testing the reliability and latency analysis under such propagation scenarios would provide some interesting results.

- In this thesis we have considered open loop massive MIMO systems, we obtained CSI at BS using UL pilot sequences. Even though we gained full spatial diversity in the absence of channel knowledge at receiver unlike conventional space-time codes like Alamouti codes. Gaining channel knowledge at BS is still a resource consuming process, investigating new strategies to adapt Unitary Space-time codes and Space-time modulation techniques into Blind Massive MIMO systems, could be an interesting research direction.

- In an indoor environment reflections and scattering in the wireless medium due to the various obstacles and reflectors results in rich-scattering multipath propagation environment. Time Reversal (TR) can take advantage of multipath propagation to treat all the scattering elements as virtual antenna systems. Single antenna TR system showed promising performance as massive MIMO systems. Implementation complexity is also affordable, this new system model is really interesting and adapting space-time codes into such systems would be an interesting research direction.

BIBLIOGRAPHY

[1] H.Ji, S.Park, J.Yeo, Y.Kim, J.Leee B.Shi m, Introduction to Ultra Reliable and Low Latency Communications in 5G,IEEE Communications Magazine, April 2017.

[2] O. N. C. Yilmaz, Y. E. Wang, N. A. Johansson, N. Brahmi, S. A. Ashraf e J. Sachs, Anal-ysis of Ultra-Reliable and Low-Latency 5G Communication for a Factory Automation UseCase, IEEE ICC - Workshop on 5G and beyond- Enabling Technolgies amd Applications, 2015.

[3] 3GPP technical specific at ion36.803 :User Equipment(EU) Transmission and Reception, Release8, V0.3.0, 3GPP, May 2007

[4] T. L. Marzetta and B. M. Hochwald, "Capacity of a mobile multiple-antenna communication link in Rayleigh flat fading," in IEEE Transactions on Information Theory, vol. 45, no. 1, pp. 139-157, Jan. 1999. doi: 10.1109/18.746779

[5] S. M. Alamouti, "A simple transmit diversity technique for wireless communications," IEEE J. Sel. Areas Commun., vol. 16, no. 8, pp. 1451-1458, Oct. 1998.

[6] S. Zhou and G. B. Giannakis, "Optimal transmitter eigen-beamforming and space-time block coding based on channel mean feedback," in IEEE Transactions on Signal Processing, vol. 50, no. 10, pp. 2599-2613, Oct. 2002. doi: 10.1109/TSP.2002.803355

[7] Shengli Zhou and G. B. Giannakis, "Optimal transmitter eigen-beamforming and space-time block coding based on channel correlations," in IEEE Transactions on Information Theory, vol. 49, no. 7, pp. 1673-1690, July 2003. doi: 10.1109/TIT.2003.813565

[8] J. Lorincz and D. Begusic, "Adaptive beamforming structure with STBC for IEEE 802.11n WLAN systems," 2008 16th International Conference on Software, Telecommunications and Computer Networks, Split, 2008, pp. 258-263.

[9] J. Joung, "Space–Time Line Code," in IEEE Access, vol. 6, pp. 1023-1041, 2018. doi: 10.1109/ACCESS.2017.2777528

[10] C. Sun, X. Q. Gao, S. Jin, M. Matthaiou, Z. Ding, and C. Xiao, "Beam-division multiple access transmission for massive MIMO communications,"IEEE Trans. Commun., vol. 63, no. 6, pp. 2170–2184, Jun. 2015.

[11] E. G. Larsson, O. Edfors, F. Tufvesson and T. L. Marzetta, "Massive MIMO for next generation wireless systems," in IEEE Communications Magazine, vol. 52, no. 2, pp. 186-195, February 2014.

[12] J. H. Winters, "Optimum combining for indoor radio systems with multiple users," IEEE Trans. Commun., vol. 35, no. 11, pp. 1222–1230, 1987.

[13] Björnson, E., M. Kountouris, M. Bengtsson, and B. Ottersten.2013b. "Receive combining vs. multi-stream multiplexing in downlink systems with multi-antenna users". IEEE Trans. Signal Process. 61(13): 3431–3446.

[14] D. Gesbert, L. Pittman, and M. Kountouris. 2006. "Transmit Correlation-Aided Scheduling in multiuser MIMO networks". In: Proc. IEEE ICASSP. Vol. 4. 249–252.

[15] Wang, H., P. Wang, L. Ping, and X. Lin. 2009. "On the impact of antenna correlation in multi-user MIMO systems with rate constraints". IEEE Commun. Lett. 13(12): 935–937.

[16] Trump, T. and B. Ottersten. 1996. "Estimation of nominal direction of arrival and angular spread using an array of sensors". Signal Processing. 50(1-2): 57–69.

[17] Yin, H., D. Gesbert, M. Filippou, and Y. Liu. 2013. "A coordinated approach to channel estimation in large-scale multiple antenna systems". IEEE J. Sel. Areas Commun. 31(2): 264– 273.

[18] Björnson, E., E. G. Larsson, and M. Debbah. 2016a. "Massive MIMO for maximal spectral efficiency: How many users and pilots should be allocated?" IEEE Trans. Wireless Commun. 15(2): 1293–1308.

[19] Gopalakrishnan, B. and N. Jindal. 2011. "An analysis of pilot contamination on multi-user MIMO cellular systems with many antennas". In: Proc. IEEE SPAWC.

[20] Jose, J., A. Ashikhmin, T. L. Marzetta, and S. Vishwanath. 2011. "Pilot contamination and precoding in multi-cell TDD systems". IEEE Trans. Commun. 10(8): 2640–2651.

[21] Rakhesh Singh Kshetrimayum, "Fundamentals of MIMO Wireless Communications", Cambridge University Press 2017

[22] P. Harris et al., "Temporal Analysis of Measured LOS Massive MIMO Channels with Mobility," 2017 IEEE 85th Vehicular Technology Conference (VTC Spring), Sydney, NSW, 2017, pp. 1-5. doi: 10.1109/VTC-Spring.2017.8108215

[23] E. Björnson, J. Hoydis, and L. Sanguinetti, "Massive MIMO networks: Spectral, energy, and hardware efficiency," Foundations and Trends in Signal Processing, vol. 11, no. 3-4, pp. 154–655, 2017. [Online]. Available: http://dx.doi.org/10.1561/2000000093

[24] John G. Proakis, "Digital Communications", McGraw-Hill, 1995.

[25] Jabbar, S.Q.; Li, Y. "Analysis and Evaluation of Performance Gains and Tradeoffs for Massive MIMO Systems". Appl. Sci. 2016, 6, 268.

[26] Ivrlac, M.T.; Nossek, J.A. "Quantifying Diversity and Correlation in Rayleigh Fading MIMO Communication Systems." In Proceedings of the 3rd IEEE International Symposium on Signal Processing and Information Technology, Darmstadt, Germany, 14–17 December 2003; pp. 158–161.

[27] Lim, A.W.C.; Lau, V.K.N. "On the Fundamental Tradeoff of Spatial Diversity and Spatial Multiplexing of MIMO Links with Imperfect CSIT." In Proceedings of the IEEE International Symposium on Information Theory, Seattle,WA, USA, 9–14 July 2006; pp. 2704–2708.

[28] A. H. Mehana and A. Nosratinia, "Diversity of MIMO Linear Precoding," in IEEE Transactions on Information Theory, vol. 60, no. 2, pp. 1019-1038, Feb. 2014. doi: 10.1109/TIT.2013.2289860

[29] Tse, D.; Viswanath, P.; Zheng, L. Diversity–Multiplexing Tradeoff in Multiple-Access Channels. IEEE Trans. Inf. Theory 2004, 50, 1859–1874.

[30] Lim, A.W.C.; Lau, V.K.N. On the Fundamental Tradeoff of Spatial Diversity and Spatial Multiplexing of MIMO Links with Imperfect CSIT. In Proceedings of the IEEE International Symposium on Information Theory, Seattle,WA, USA, 9–14 July 2006; pp. 2704–2708.

[31] C. Sun, X. Q. Gao, S. Jin, M. Matthaiou, Z. Ding, and C. Xiao, "Beam-division multiple access transmission for massive MIMO communications,"IEEE Trans. Commun., vol. 63, no. 6, pp. 2170–2184, Jun. 2015.

[32] V. Tarokh, H. Jafarkhani, and A. R. Calderbank, "Space-time block-codes from orthogonal designs,"IEEE Trans. Inf. Theory, vol. 45, no. 5,pp. 1456–1467, Jul. 1999

[33] Runhua Chen, J. G. Andews and R. W. Health, "Multiuser space-time block coded MIMO with downlink precoding," 2004 IEEE International Conference on Communications (IEEE Cat. No.04CH37577), Paris, France, 2004, pp. 2689-2693 Vol.5.

[34] J. Joung, "Space–Time Line Code for Massive MIMO and Multiuser Systems With Antenna Allocation," in IEEE Access, vol. 6, pp. 962-979, 2018. doi: 10.1109/ACCESS.2017.2777102

[35] Krishnamoorthy, A. and D. Menon. 2013. "Matrix inversion using Cholesky decomposition". In: Proc. Alg. Arch. Arrangements Applicat. 70–72.

[36] Ingemarsson, C. and O. Gustafsson. 2015. "On fixed-point implementation of symmetric matrix inversion". In: Proc. ECCTD. 1–4.